

AD-A075 854

SWEDISH STATE SHIPBUILDING EXPERIMENTAL TANK GÖTEBORO  
SUPERCAVITATING PROPELLER PERFORMANCE. INFLUENCE OF PROPELLER G--ETC(U)  
1978 O RUTQERSSON

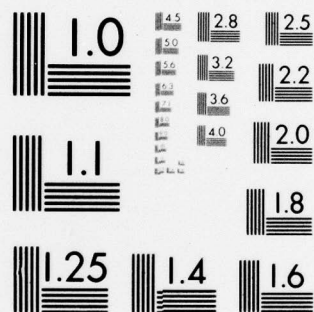
F/6 13/10  
1978 O RUTQERSSON

UNCLASSIFIED

NL

1 OF 1  
AD  
A075854





MICROCOPY RESOLUTION TEST CHART  
NATIONAL BUREAU OF STANDARDS-1963-A

AD A075854

241 S

311 MR

then DDC

MEDDELANDEN

FRÅN

STATENS SKEPPSPROVNINGSANSTALT

(PUBLICATIONS OF THE SWEDISH STATE SHIPBUILDING EXPERIMENTAL TANK)

Nr 82

GÖTEBORG

1979

1  
B S

**SUPERCAVITATING PROPELLER PERFORMANCE.  
INFLUENCE OF PROPELLER GEOMETRY  
AND INTERACTION  
BETWEEN PROPELLER, RUDDER AND HULL**

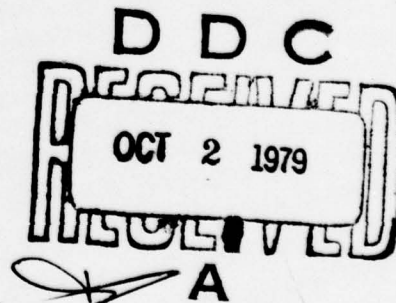
BY

**OLLE RUTGERSSON**

Extended version of paper presented at the  
Joint Symposium on Design and Operation of  
Fluid Machinery

Fort Collins, Colorado, USA  
June 12-14, 1978

DDC FILE COPY



79 09 27 061

*Meddelanden från*  
**STATENS SKEPPSPROVNINGSANSTALT**

1. Statens Skeppsprovsningsanstalt (Historik, allmän planering, kostnader, Principer, allmän beskrivning; Några synpunkter på byggnadsproblemet; Rännans konstruktion och utförande; Den instrumentella utrustningen; Den elektriska utrustningen; Uppgifter, organisation) [Summary in English], av HUGO HAMMAR, H.F. NORDSTRÖM, M. WERNSTEDT, SVEN HULTIN, R. RÖDSTRÖM, KARL TISELIUS, 1942.
2. Försök med fiskebåtsmodeller [Tests with Fishing Boat Models, Summary in English] av H.F. NORDSTRÖM, 1943.
3. Experiments with Bulbous Bows, av ANDERS LINDBLAD, 1944.
4. Propellers with Adjustable Blades, av H.F. NORDSTRÖM, 1945.
5. Nogle Praktiske og Teoretiske Undersøgelser om Modelpropellere [Some Practical and Theoretical Investigations of Model Propellers, Summary in English], av JØRGEN MARSTRAND, 1945.
6. The Effect of the Air Content of Water on the Cavitation Point and upon the Characteristics of Ships' Propellers, av HANS EDSTRAND, 1946.
7. Modellförsök med en färje [Model Tests with a small Ferry, Summary in English], av H.F. NORDSTRÖM och E. FREIMANIS, 1947.
8. Further Experiments with Bulbous Bows, av ANDERS LINDBLAD, 1948.
9. Screw Propeller Characteristics, av H.F. NORDSTRÖM, 1948.
10. Some Systematic Tests with Models of Fast Cargo Vessels, av H.F. NORDSTRÖM, 1948.
11. The Electrical Equipment of the Swedish State Shipbuilding Experimental Tank, av KARL TISELIUS, 1949.
12. The Resistance of a Barge with the Bottom Air Lubricated, av HANS EDSTRAND och RAGNAR RÖDSTRÖM, 1949.
13. Medstrømskoefficientens Afhængighed af Rorform, Trim og Hækbølge [The Dependence of Wake on Shape of Rudder, Trim and Stern Wave, Summary in English], av SVEND AAGE HARVALD, 1949.
14. Further Tests with Models of Fast Cargo Vessels, av H.F. NORDSTRÖM, 1949.
15. Cavitation Tests with Model Propellers in Natural Sea Water with Regard to the Gas Content of the Water and its Effect upon Cavitation Point and Propeller Characteristics, av HANS EDSTRAND, 1950.
16. Systematic Tests with Models of Cargo Vessels with  $\delta_{pp}=0.575$ , av H.F. NORDSTRÖM, 1950.
17. Propulsion Problems Connected with Ferries, av H.F. NORDSTRÖM och HANS EDSTRAND, 1951.
18. Model Tests with Turbulence Producing Devices, av H.F. NORDSTRÖM och HANS EDSTRAND, 1951.
19. Some Tests with Models of Small Vessels, av H.F. NORDSTRÖM, 1951.
20. Model Tests with Icebreakers, av H.F. NORDSTRÖM, HANS EDSTRAND och HANS LINDGREN, 1952.
21. Om djupgåendets inflytande på propulsionegenskaperna [The Influence of Draught on Propulsive Qualities, Summary in English], av HANS EDSTRAND, 1952.
22. Model Tests on the Optimum Diameter for Propellers, av HANS EDSTRAND, 1953.
23. Experiments with Tanker Models I, av HANS EDSTRAND, E. FREIMANIS och HANS LINDGREN, 1953.
24. Några systematiska försök med modeller av mindre kustfartyg [Tests with Models of Coasters, Summary in English], av AXEL O. WARHOLM, 1953.
25. The Transverse Stability and Resistance of Single-Step Boats when Planing, av R. RÖDSTRÖM, HANS EDSTRAND och H. BRATT, 1953.
26. Experiments with Tanker Models II, av HANS EDSTRAND, E. FREIMANIS och HANS LINDGREN, 1953.
27. Full Scale Tests with the »Wrangel» and Comparative Model Tests, av H.F. NORDSTRÖM, 1953.
28. On Propeller Scale Effects, av H.F. NORDSTRÖM, HANS EDSTRAND och HANS LINDGREN, 1954.
29. Experiments with Tanker Models III, av HANS EDSTRAND, E. FREIMANIS och HANS LINDGREN, 1954.
30. Resistance Experiments with Divided Ship Models, av R. RÖDSTRÖM, 1954.
31. On the Influence of Form upon Skin Friction Resistance, av H.F. NORDSTRÖM, HANS EDSTRAND och HANS LINDGREN, 1954.
32. Statens Skeppsprovsningsanstalt (The Swedish State Shipbuilding Experimental Tank) in Göteborg. A Short Account of the Establishment, its Work, Equipment and Organisation, av H.F. NORDSTRÖM, 1954.
33. The Influence of Propeller Clearance and Rudder upon the Propulsive Characteristics, av H. LINDGREN, 1955.
34. Seventh International Conference on Ship Hydrodynamics; Reports, Discussions and Conclusions, av H.F. NORDSTRÖM och HANS EDSTRAND, 1955.
35. Further Tests with Models of Coasters, av HANS LINDGREN och AXEL O. WARHOLM, 1955.
36. Experiments with Tanker Models IV, av HANS LINDGREN, 1956.
37. Experiments with Tanker Models V, av HANS EDSTRAND, E. FREIMANIS och HANS LINDGREN, 1956.
38. Systematic Tests with Models of Ships with  $\delta_{pp}=0.525$ , av HANS EDSTRAND och HANS LINDGREN, 1956.
39. Systematic Tests with Ship Models with  $\delta_{pp}=0.675$ , Part I, av E. FREIMANIS och HANS LINDGREN, 1957.
40. Tests with Geometrically Similar Models of the Victory Ship, av HANS LINDGREN och E. BJARNE, 1957.
41. Systematic Tests with Ship Models with  $\delta_{pp}=0.675$ , Part II, av E. FREIMANIS och HANS LINDGREN, 1957.
42. Systematic Tests with Ship Models with  $\delta_{pp}=0.675$ , Part III, av E. FREIMANIS och HANS LINDGREN, 1958.
43. The Cavitation Laboratory of the Swedish State Shipbuilding Experimental Tank, av HANS LINDGREN, 1958.
44. Systematic Tests with Ship Models with  $\delta_{pp}=0.600-0.750$ , av E. FREIMANIS och HANS LINDGREN, 1959.
45. A Study of Course Keeping and Manoeuvring Performance, av NILS H. NORRBIN, 1960.
46. The Correlation of Ship Power and Revolutions with Model Test Results, av HANS LINDGREN och C.-A. JOHNSON, 1960.

Forts. å omslagets 3:e sida [Continued on inside back cover].



MEDDELANDEN

FRÅN

STATENS SKEPPSPROVNINGSANSTALT

(PUBLICATIONS OF THE SWEDISH STATE SHIPBUILDING EXPERIMENTAL TANK)

Nr 82

GÖTEBORG

1979

6  
**SUPERCAVITATING PROPELLER PERFORMANCE.  
INFLUENCE OF PROPELLER GEOMETRY  
AND INTERACTION  
BETWEEN PROPELLER, RUDDER AND HULL,**

BY

10 **OLLE/RUTGERSSON**

Extended version of paper presented at the  
Joint Symposium on Design and Operation of  
Fluid Machinery

Fort Collins, Colorado, USA  
June 12-14, 1978



Accession For	
NTIS GRA&I	<input checked="checked" type="checkbox"/>
DDC TAB	<input type="checkbox"/>
Unannounced	<input type="checkbox"/>
Justification	
By	
Distribution/	
Availability Codes	
Dist..	Availand/or special
A	A

338 000

*Distributed by:*  
Liber Distribution  
S-162 89 VÄLLINGBY Sweden  
ISBN 91-38-04946-5  
ISSN 0373-4714

## CONTENTS

	PAGE
SUMMARY	2
RESUME	2
1. INTRODUCTION	3
2. NOTATION	3
3. PROPELLER GEOMETRY	5
4. DESIGN PROCEDURE	8
5. TEST PROCEDURE	9
6. TEST RESULTS	9
7. CAVITATION PROPERTIES	13
8. CORRECTION OF DESIGN PROCEDURE	15
9. INFLUENCE OF DESIGN PARAMETERS	17
10. COMPARISON WITH OTHER PROPELLERS	20
11. INFLUENCE OF PROFILE SHAPE	23
12. INFLUENCE OF SHAFT INCLINATION AND CLEARANCES TO BOTTOM AND RUDDER	28
12.1 INFLUENCE OF SHAFT INCLINATION	28
12.2 INFLUENCE OF VERTICAL CLEARANCE	28
12.3 INFLUENCE OF RUDDER ARRANGEMENT	31
12.4 INTEGRATED EFFECT	34
13. COMPARISON WITH FULL SCALE OBSERVATIONS	34
14. MEASUREMENTS OF PRESSURE FLUCTUATIONS	38
15. CONCLUSIONS	39
16. ACKNOWLEDGEMENTS	40
17. REFERENCES	40
APPENDIX	
GEOMETRY AND CHARACTERISTICS OF THE PARENT SERIES	42

79 09 27 061

## SUMMARY

Systematic tests with supercavitating propellers have been carried out. The results are shown as design charts, performance curves, cavitation limits and empirical corrections of the design method.

Influence on the performance of profile modifications, shaft inclination and interaction between propeller, rudder and hull is shown.

Cavitation observations and measurements of thrust, torque and pressure fluctuations at model tests are compared with corresponding measurements in full scale.

## RESUME

On a mis à l'épreuve une série des hélices supercavitantes. Les résultats principaux sont présentés sur des diagrammes de conception, des courbes de performance propulsif, des contours de régimes différents de cavitation et des facteurs de corrections pour la méthode théorique de calcul de conception d'une hélice.

L'influence sur le performance d'une modification de la forme de profile, d'une inclination de l'arbre et l'interaction hélice-gouvernail et hélice-coque est mise en évidence.

Les figures de cavitation, les caractéristiques globales et les fluctuations de pression sur la coque obtenues sur modèle sont comparées avec les résultats correspondants obtenus à la mer.



## 1. INTRODUCTION

The Swedish interest in supercavitating propellers started in the late 1950s. Some early designs showed that the design procedures for such propellers were less accurate than the design methods for conventional propellers. The information was also rather scarce on the influence of parameters such as blade area ratio, hub diameter and design thrust on propeller performance. To increase the knowledge in this area a systematic investigation of supercavitating propellers was started at SSPA, sponsored by the Defence Material Administration of Sweden. Since the Swedish SPICA-class torpedo boats are fitted with supercavitating propellers, the research work has later been extended to include also correlation studies between model- and full scale tests.

## 2. NOTATION

$A(X_1)$	= coefficient for camber distribution
$C(X_1)$	= coefficient for thickness distribution
$C_L$	= lift coefficient = $C_{L0} + C_{L\alpha}$
$C_{L0}$	= camber part of lift coefficient
$C_{L\alpha}$	= angle of attack part of lift coefficient
$D$	= propeller diameter
$D(X_1)$	= coefficient for thickness distribution
$J$	= $V_A/n \cdot D$ = advance ratio
$J_F$	= advance ratio for incipient face cavitation at $\sigma = 0.6$
$J_{SC}$	= advance ratio for supercavitation at $\sigma = 0.6$
$K_P$	= $2p/\rho n^2 D^2$ = dimension-less pressure amplitude
$K_T$	= $T/\rho n^2 D^4$ = thrust coefficient
$K_Q$	= $Q/\rho n^2 D^5$ = torque coefficient
$l$	= profile length



4

### 3. PROPELLER GEOMETRY

The starting point for the series was a parent propeller designed for

$$J = 0.814$$

$$K_T = 0.113$$

$$\sigma = 0.58$$

The blade area ratio for this propeller was chosen as a compromise between a small wetted surface and small angles of attack for the profiles. The conflict between these two demands is to some extent illustrated by equation (1). The profile thickness is here expressed as a lift part and an angle of attack part [2].

$$t(x_1) = C_L lC(X_1) + \alpha lD(X_1) \quad (1)$$

The first term of the equation is independent of the blade area ratio. In the second term, however, it is necessary to increase the angle of attack if a smaller blade area is chosen and the thickness is kept constant. A larger angle of attack means a higher drag, thus a smaller blade area ratio does not always give a lower drag. In Fig 1 the blade shape of the parent series is shown together with some other shapes considered.

The propellers were designed with a wedge shaped profile as this was considered to have the best performance. Thus the "three term" distribution was chosen for the face. The "three term" thickness distribution was considered to give too thin leading edges so the TMB "two term modified" thickness distribution was chosen for the series [2]. A "three term modified" distribution should of course have been more appropriate to a "three term" face. The designation is however believed to be of less importance once one has left the theoretical distribution.

Until now nine propeller models, including the parent propeller, have been designed and tested at SSPA. Some data for the propellers are shown in Table 1.

The basic series is an advance ratio variation of the parent propeller. Other parameters investigated were hub diameter, thrust coefficient and blade area ratio. The propellers representing these latest variations were manufactured with adjustable pitch and tested at several pitch settings.

	$A_D/A_0$	$X_h$	
————	0.5	0.2	SSPA parent
————	0.6	0.3	KMW Spica I
-----	0.5	0.16	Newton-Rader [1]
.....	0.4	0.2	Venning-Haberman [2]

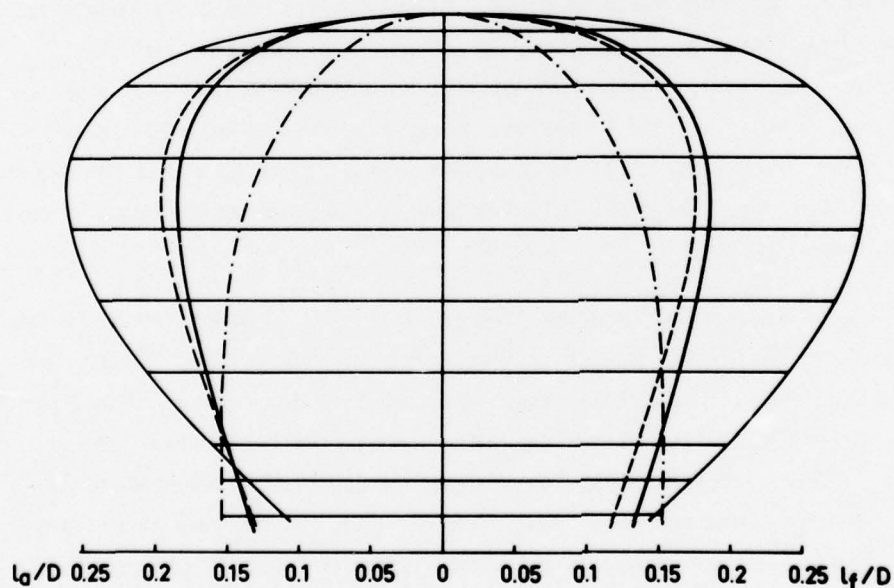


Fig 1. Comparison of different blade shapes

Prop No	Design point			$A_D/A_O$	$X_h$	Adj pitch	Tested at $P_{0.7D}$
	J	$K_T$	$\sigma$				
P1426	0.814	0.113	0.58	0.5	0.19	No	1.166
P1439	1.15	"	"	"	"	No	1.446
P1440	1.6	"	"	"	"	No	1.74
P1441	0.6	"	"	"	"	No	0.982
P1411	0.814	"	"	"	0.3	Yes	1.005 1.185 1.440 1.7 2.0
P1436	0.814	0.05	"	"	0.19	No	0.97
P1478	"	0.18	"	"	"	Yes	1.0 1.1 1.2 1.4 1.7
P1428	"	0.113	"	0.6	"	No	0.953
P1693	"	"	"	0.6	"	Yes	1.144 1.440 1.70

Table 1. Extent of propeller series



#### 4. DESIGN PROCEDURE

The design procedure follows the method outlined in [2,4]. Thus the radial lift distribution is calculated by the Goldstein  $\kappa$ -method [3] using an optimum circulation distribution. The blade sections are then designed according to equations (1) and (2).

$$y/l = A(X_1)C_{L0}/k_1 \quad (2)$$

The thicknesses are also determined by the demand for adequate strength. For all propellers in the series the maximum stress level calculated by the beam theory [4] is  $100 \text{ N/mm}^2$  at the design load for a fullscale propeller with a diameter of 1.2 m.

The lifting surface camber corrections  $k$  according to Ludwig-Ginzel are taken from [5].

The final pitch distribution is then calculated with equation (3).

$$P/D = \pi x \tan(\beta_1 + \alpha) - \left[ \Delta(P/D)C_{\sigma} \right] \quad (3)$$

where  $\Delta(P/D)C_{\sigma}$  are corrections due to non zero cavitation number [2].



## 5. TEST PROCEDURE

All tests were carried out in the high speed test section of the cavitation tunnel No 2 at SSPA [6]. The propellers were located upstream of the "z-drive" dynamometer. Tests were performed in homogenous flow and at 8 degrees shaft inclination. The propeller models were tested at 11 cavitation numbers in homogeneous flow  $\sigma = 0.25, 0.3, 0.4, 0.5, 0.6, 0.7, 0.8, 1.0, 1.5, 2.0$  and at 3 atm absolute pressure in the tunnel. The water speed was kept as high as was possible from power limitations. Thus most of the tests were run at 11 m/s, but also 9 m/s and 7.5 m/s were used at high cavitation numbers. The air content of the water was kept constant throughout the series of tests at about 40 per cent of saturation ( $\alpha/\alpha_s = 0.4$ )

The cavitation patterns on the face and the back of the blades were photographed at four different advance ratios at each cavitation number.

## 6. TEST RESULTS

At the analysis of the test results the main interest was devoted to cavitation numbers around  $\sigma = 0.6$ . Thus design charts were made for  $\sigma = 0.6$  for the parent series (Fig 3) and for the three propellers with adjustable pitch. For the parent series design charts were also made for  $\sigma = 0.4$  and 0.8 (Figs 2,4).

The propeller characteristics which form the basis for the design charts in Figs 2-4 are shown in the Appendix. Further, these characteristics have been interpolated from the results for the four tested propellers of the parent series. This interpolation was made by hand, as attempts to do the work by regression analysis and by Lerbs' equivalent profile method were unsuccessful.



10

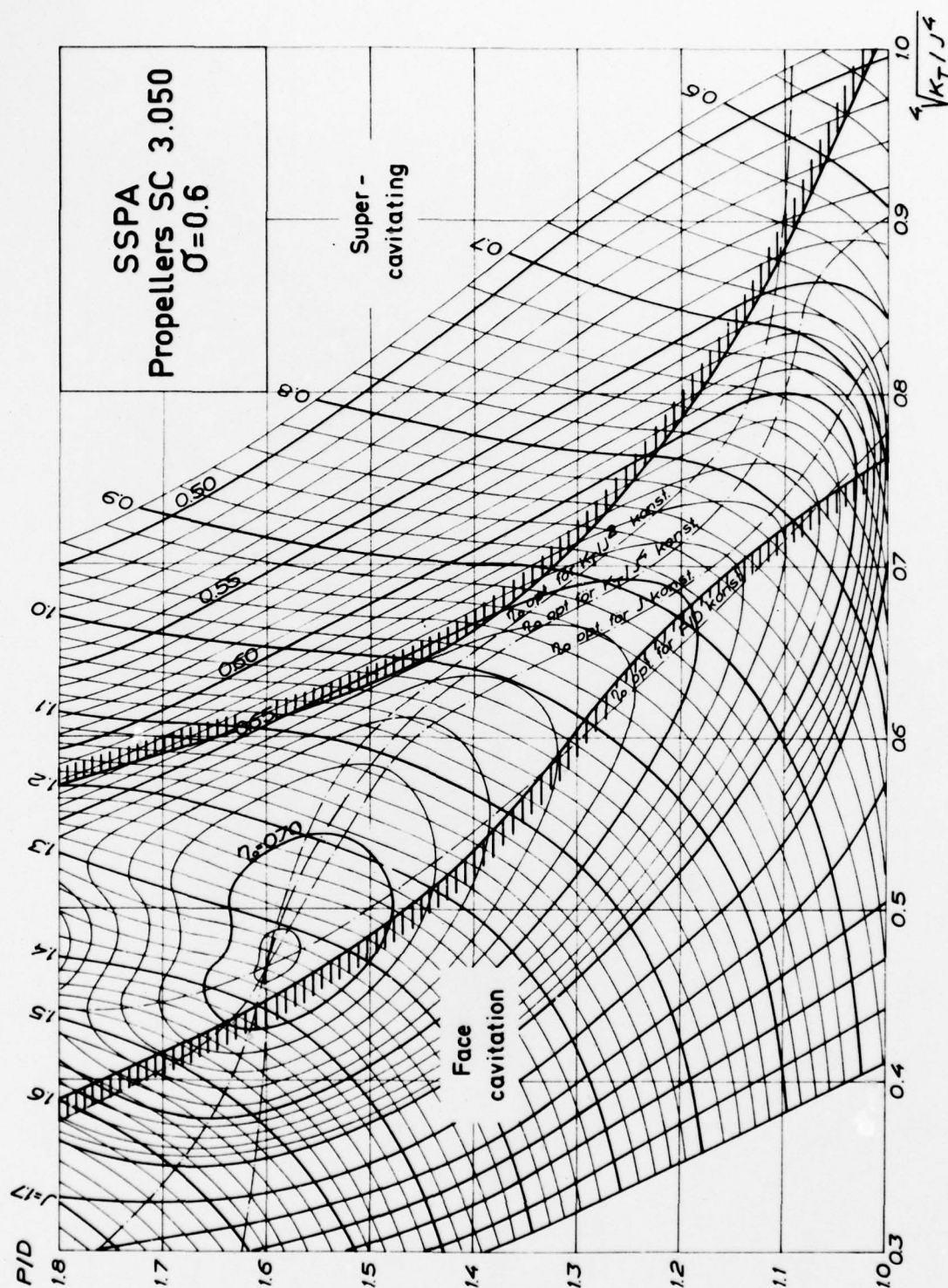


Fig 3. Design chart for the parent series,  $\sigma = 0.6$





## 7. CAVITATION PROPERTIES

When designing a propeller it is important to be able to estimate the cavitation behaviour of the propeller. First, the risk for erosion can often be estimated from the cavitation type and secondly, the way of improving the design is dependent on the cavitation pattern.

Face cavitation is very erosive and should be avoided, if possible. The limits for incipient face cavitation for the propeller series have been determined by studying the cavitation photographs. In Figs 2-4 the limits for the parent series are shown as shaded curves. Fig 5 shows an attempt to give the limits for all the tested propellers in one diagram. The advance ratio for incipient face cavitation was almost independent on the cavitation number for  $\sigma < 0.8$ . This result was also shown by Newton-Rader [1]. Thus the curves of Fig 5 are valid for  $0.4 < \sigma < 0.8$ . The simple parameters show a rather small dispersion for the design pitch.

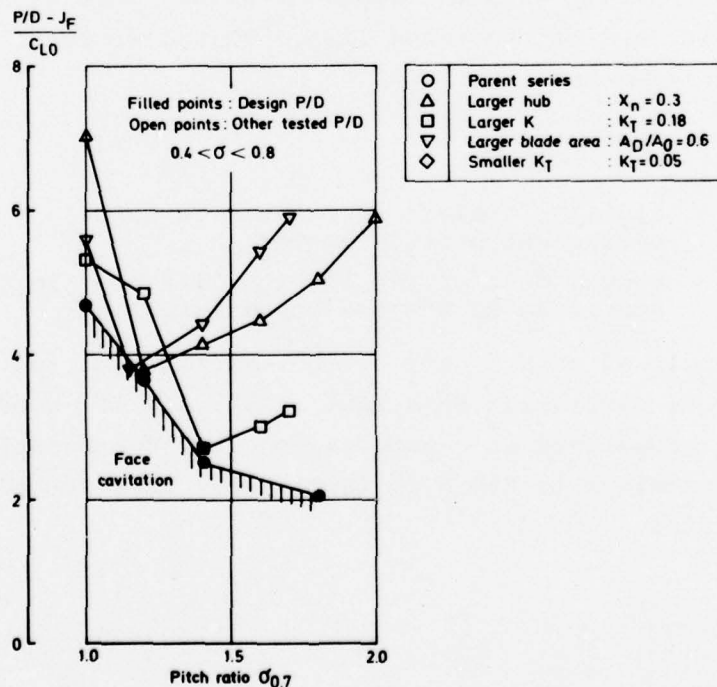


Fig 5. Conditions for incipient face cavitation



The propellers which were tested at other pitch settings than the design pitch show that the best margin against face cavitation is obtained at design pitch. It is obviously important to have the correct pitch distribution in order to avoid face cavitation. Thus the risk for face cavitation on controllable pitch propellers is very pronounced.

Attempts have also been made to find parameters defining the conditions when the propellers are supercavitating.

In this case, the propeller is considered as supercavitating when the sheet cavitation starting at the leading edge is extended beyond the trailing edge. This is the working condition for which the propeller is designed. Thus the risk for erosion is very small. First the lift coefficients calculated by Lerbs' equivalent profile method for the supercavitating conditions were plotted against the local cavitation number at radius 0.7 of the propeller radius. The scatter of the points was, however, considerable. A smaller dispersion was achieved when the angle of attack part of the lift was used instead of the total lift. This lift coefficient was calculated as:

$$C_{L\alpha} = C_L - C_{Lo} \quad (4)$$

where

$C_L$  = lift coefficient calculated by Lerbs' equivalent profile method

$C_{Lo}$  = camber part of the profile lift coefficient according to the design calculations

In Fig 6 the angle of attack part of the lift is plotted against the local cavitation number at radius 0.7 for conditions when the propellers were supercavitating. The relation between the parameters in Fig 6 is fairly well represented by a straight line.

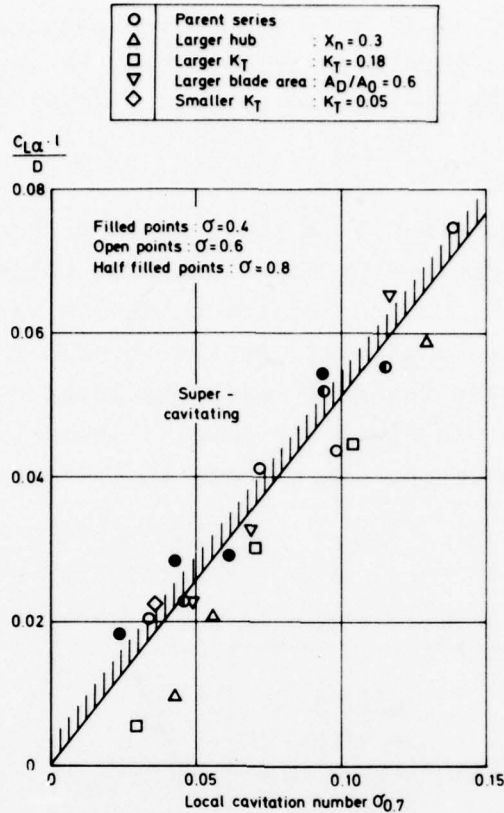


Fig 6. Conditions for supercavitation

## 8. CORRECTION OF DESIGN PROCEDURE

As pointed out in [2] the main drawback with the design method used is that the cavitation extension is not estimated. As a result of this, a partially cavitating propeller designed according to this method will match the design conditions well. On the other hand, a supercavitating propeller will be considerably underpitched because of cavity-blade interference. More modern design methods [7] account for this effect.

By use of the design charts made for the tested propellers a pitch correction complementary to that of Eq (3) can be estimated. Such a correction is shown in Fig 7. The para-

meter used is based on ideas on the cavity-blade interference outlined in [8] and is inversely proportional to the gap between the upper surface of the cavity and the face of the next blade.

In [8] this gap to chord ratio is shown to be proportional to the advance ratio divided by the blade area ratio. To get the parameter of Fig 7, the cavity thickness was then assumed to increase proportionally to the squared thrust coefficient and increase inversely with the local cavitation number at radius 0.7. In Fig 7 all results (except that for the propeller with larger hub) are shown to follow the same curve.

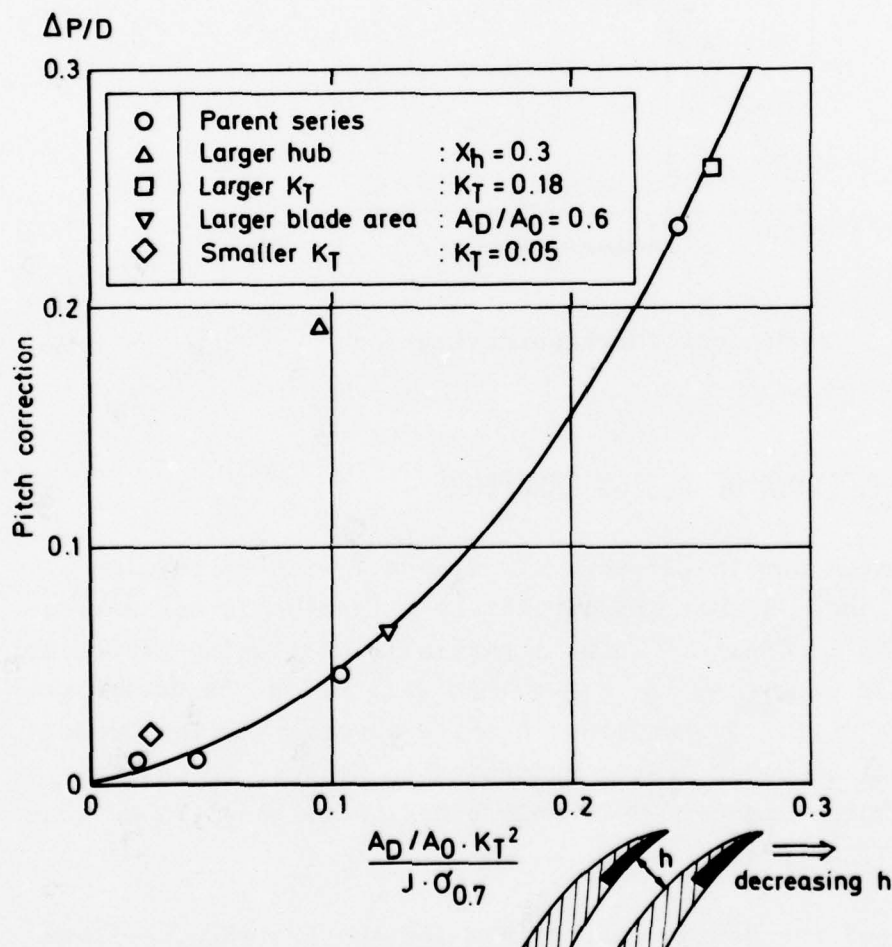


Fig 7. Pitch correction for blade cavity interference

Using this curve, the final pitch for the propeller should be:

$$P/D = \pi \tan(\beta_1 + \alpha) - \left[ \Delta(P/D) \cdot C_o \right] + \Delta P/D \quad (5)$$

where the last term is the correction for cavity-blade interference.

## 9. INFLUENCE OF DESIGN PARAMETERS

One of the main purposes with the systematic series was to investigate the influence on propeller performance of different design parameters. In Figs 8 and 9 the efficiencies for the tested propellers are compared on the basis of  $\sqrt[4]{K_T}/J$ . Two criteria are used, namely the maximum efficiency for constant  $K_T/J$  and the efficiency at the conditions for supercavitation. The reason for these two comparisons is that the cavitation pattern of the propeller is very important. Many propellers have unfavourable cavitation (face cavitation) at maximum efficiency. At the point of supercavitation the risk for erosion on the blades is however very small. This is therefore a more fair point of comparison, especially when comparing supercavitating propellers with more conventional propellers.

The comparisons are made for cavitation numbers  $\sigma = 0.4$  and  $0.6$ . Also the thrust coefficients are compared in order to give a view of the difference in propeller diameter. In Figs 8 and 9 the parent series is shown to have the best efficiency in all diagrams and over almost the whole range of  $\sqrt[4]{K_T}/J$ . At very high propeller loadings the propeller with higher blade area ratio is somewhat more favourable.



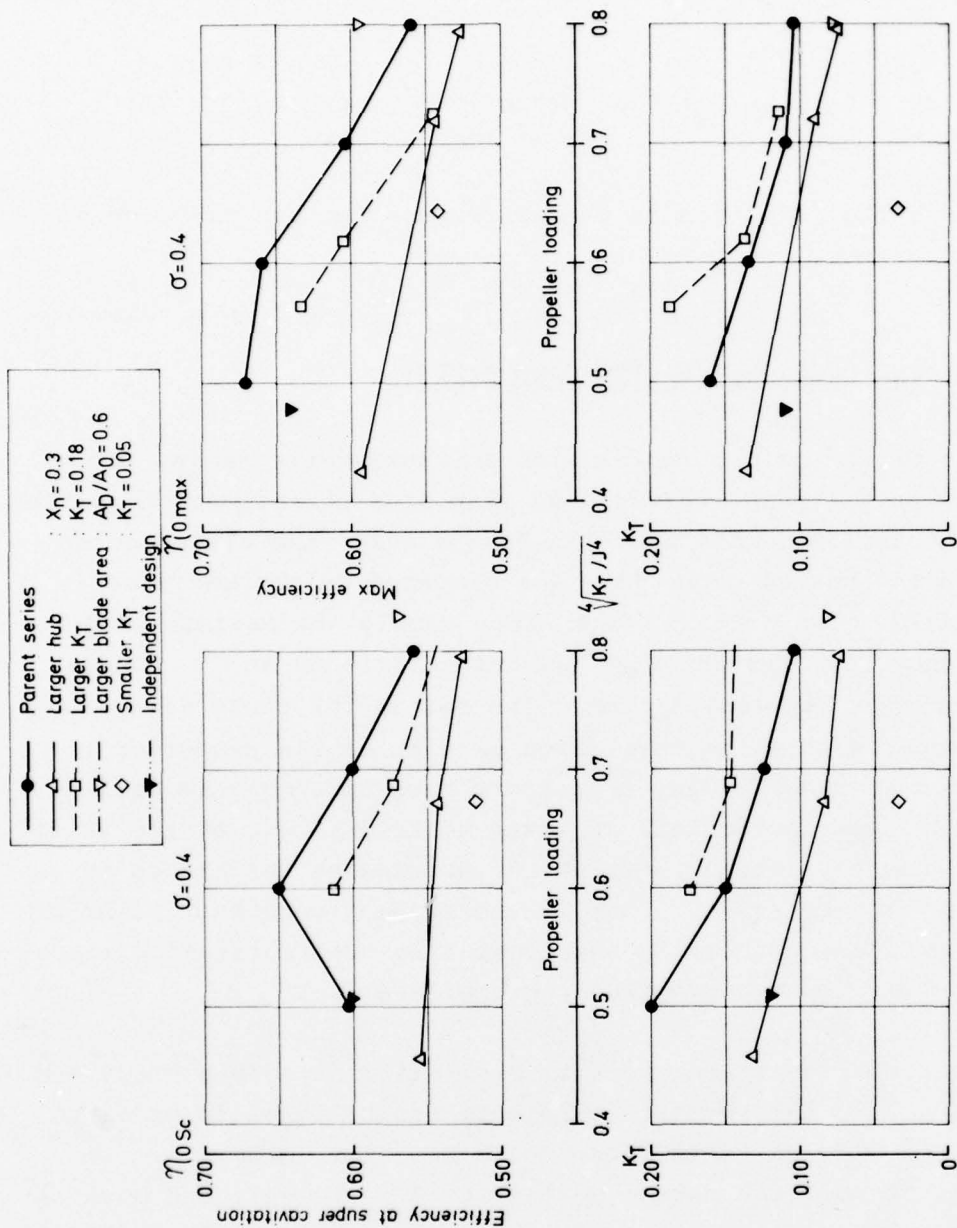


Fig 8. Influence of design parameters on thrust and efficiency,  $\sigma = 0.4$



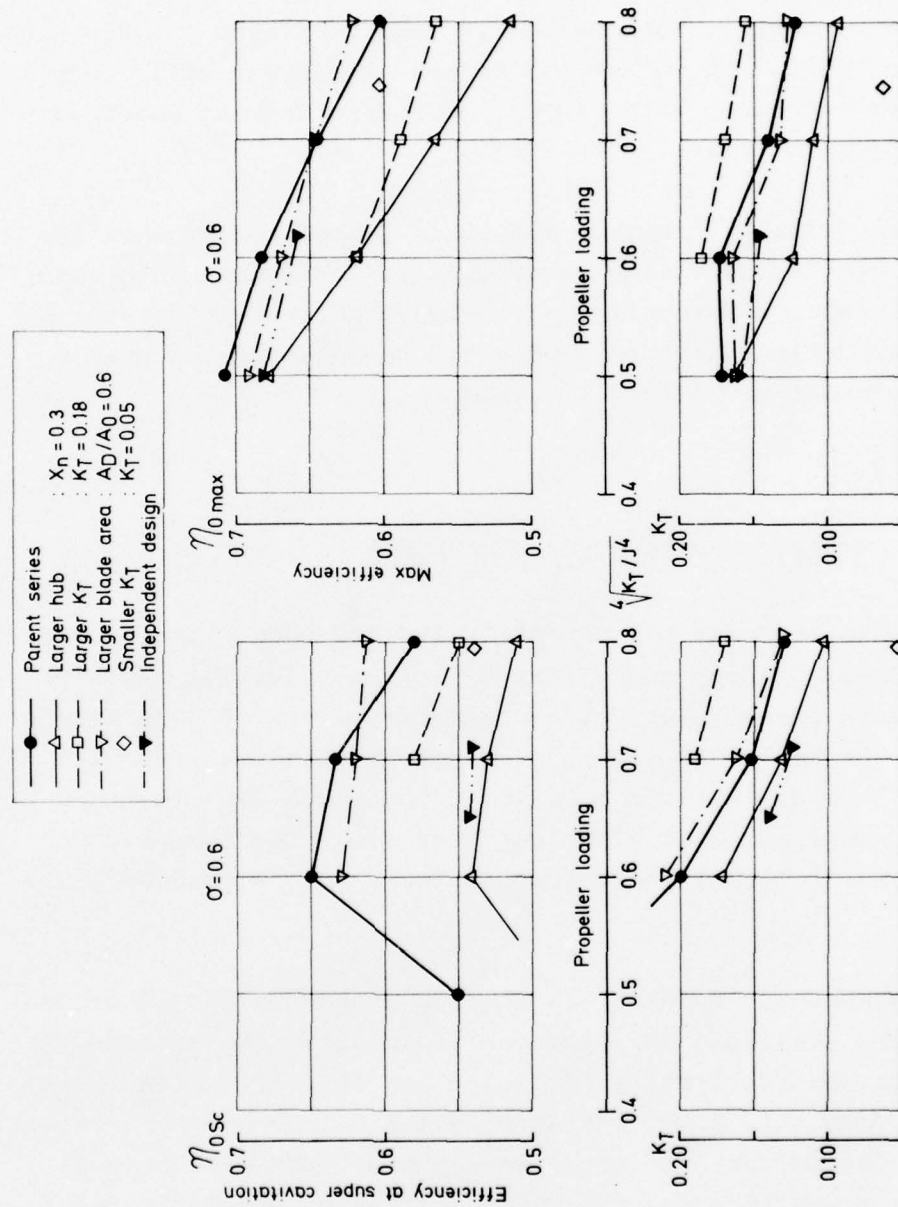


Fig 9. Influence of design parameters on thrust and efficiency,  $\sigma = 0.6$

In Figs 8 and 9 results for a propeller ( $A_D/A_O = 0.6 \times h = 0.3$ ) independent of the series are also shown. This propeller appears to have lower efficiency than the propeller in the series with blade area ratio 0.6 (but hub ratio = 0.2). Also the hub variation within the series gave lower efficiency for the propeller with larger hub, especially at supercavitating conditions at  $\sigma = 0.6$ .

The propeller with higher and lower design thrust than the parent series have also lower efficiency in the whole loading range. The propeller with higher thrust has however a smaller optimum diameter and could be advantageous when a very compact propeller is needed.

## 10. COMPARISON WITH OTHER PROPELLERS

The performance of the parent series has been compared with both the high speed propellers of Newton-Rader [1] and with some more conventional high speed propellers of SSPA design [9]. The SSPA propellers have Naca 16 thickness and Naca  $a = 0.8$  mean lines and a radial circulation distribution with rather unloaded blade root and tip. The comparison is shown in Figs 10 and 11 in the same way as in Figs 8 and 9.

Photographs of propeller cavitation on Newton-Raders propellers are available only for one propeller. The advance ratio for supercavitating condition has therefore been estimated from the torque characteristics as the point where  $k_Q$  is almost independent of advance ratio. For SSPA conventional propellers the cavitation extension was estimated from photographs. The method used for Newton-Raders propellers was however used also for the SSPA propellers as a test of the method. The agreement between the " $k_Q$ -method" and the "photograph-method" was found to be rather good.

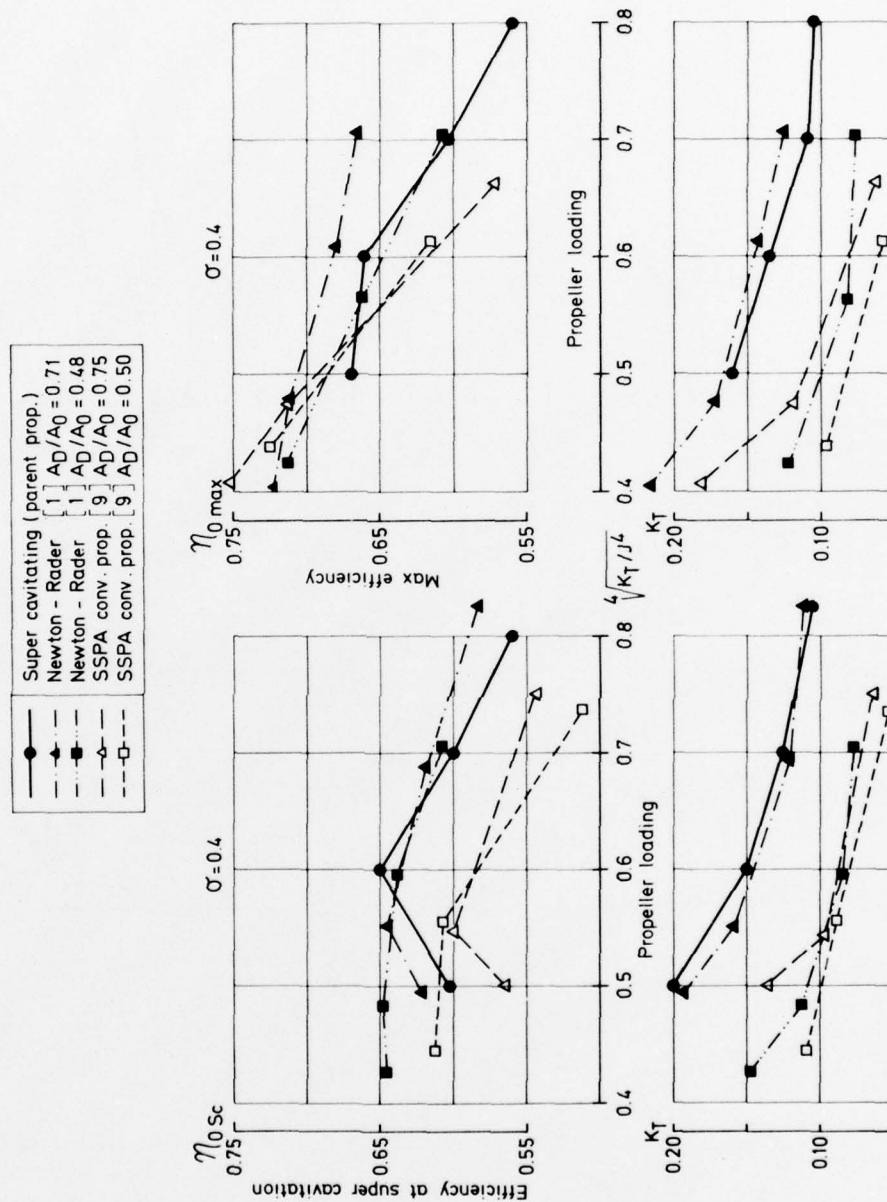


Fig 10. Comparison of thrust and efficiency with other propeller series,  $\sigma = 0.4$

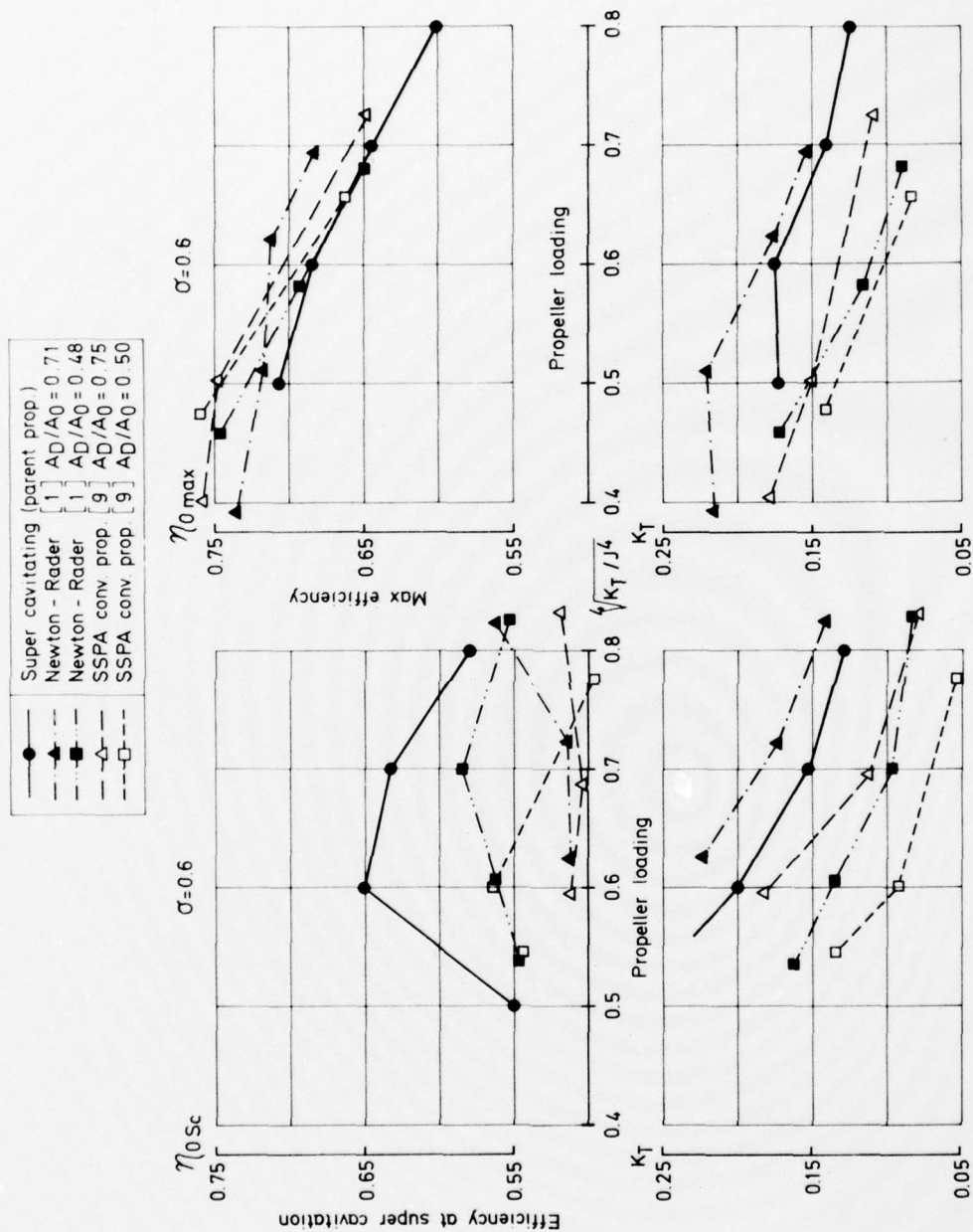


Fig 11. Comparison of thrust and efficiency with other propeller series,  $\sigma = 0.6$



The maximum efficiency for the different series is shown to lie in a very narrow range, especially at  $\sigma = 0.6$ . For medium and high loadings the Newton-Rader propellers of  $A_D/A_O = 0.71$  have the highest efficiency. When supercavitating on the other hand the parent series has about the same efficiency at  $\sigma = 0.4$  and a much better efficiency than Newton-Raders propellers at  $\sigma = 0.6$ . The propellers of conventional design have, as expected, low efficiencies when supercavitating. The thrust coefficient is also very low for these propellers.

For high speed propellers working on inclined shaft, root erosion is a serious problem [10]. Erosion tests in the cavitation tunnel using the paint technique for the parent propeller on 8 degrees inclined shaft did not however show root erosion in any loading condition. The supercavitating propeller is therefore believed to be advantageous also at rather high cavitation numbers, when an erosion free propeller is important.

## 11. INFLUENCE OF PROFILE SHAPE

The thickness for the propeller series was chosen according to the TMB two-term modified distribution [2] where the thickness in the leading edge part of the profile has been increased relative to the Tulin two-term distribution in order to increase the profile strength. The influence of this thickening of the profiles was investigated on one propeller.

To improve the backing characteristics of the propeller a modified trailing edge was also tested.

The modifications were carried out on the parent propeller and tested in two steps. First the trailing edge was made more profile like on the back side, according to Fig 12. Then the fore part of the backside was made thinner to agree with the Tulin two-term thickness distribution. The results of the tests in the normal range of advance ratios are shown

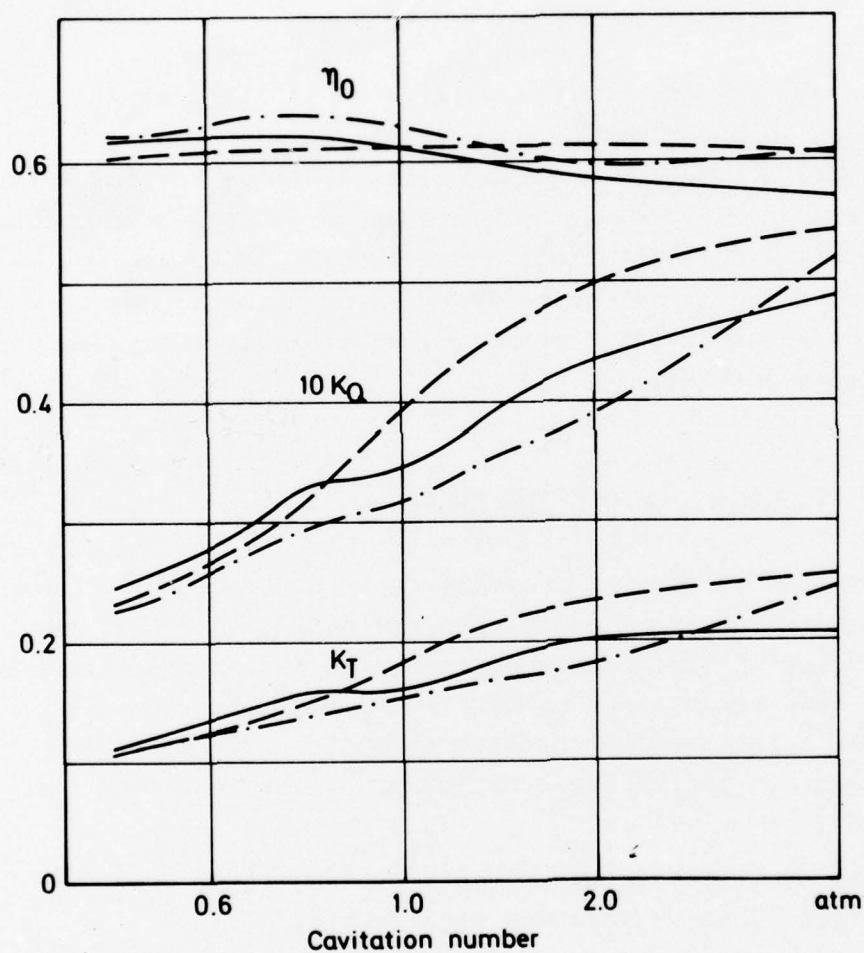
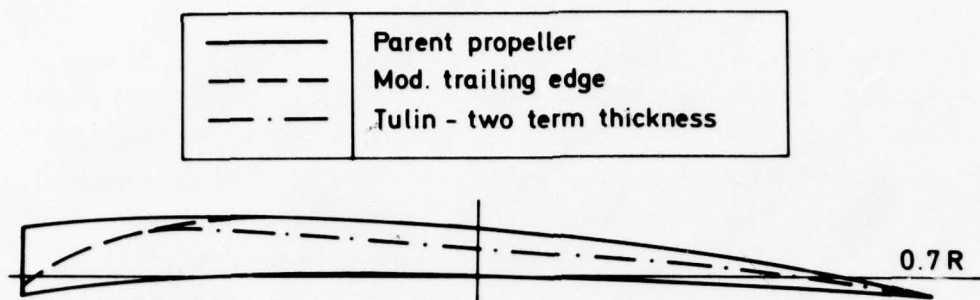


Fig 12. Effect of profile modification on propeller characteristics at  $J = 0.8$

in Fig 12. It is evident that the profiled trailing edge improved the propeller performance in the low speed range. The reason for this is probably a larger mean line camber and a smaller separation zone due to this modification. It is interesting to note that the high speed performance is only slightly inferior to that of the original profile.

The Tulin two-term profile is shown to improve the efficiency in the high speed range. The improvement is, however, moderate considering the rather large reduction of the profile thickness.

In Fig 13 the stresses in the blade are shown to increase about 100% when the thickness distribution is changed from "two-term modified" to "original two-term". These stresses were calculated using a finite element method [11].

Fig 14 shows the complete distribution of the principal stresses on the suction side of the parent propeller with the original two-term thickness distribution. The maximum stresses are shown in the root sections. The elements near the leading edge have positive stresses on both sides. Thus the fore part of the blade is working as a shell and the loads are transformed into membrane stresses. This is probably the reason for the rather moderate bending stresses in the blade. In [17] the maximum stresses in a supercavitating propeller blade is shown to appear about 20% of the chord length from the leading edge at radius 0.7. In order to achieve this calculations on the parent propeller have also been carried out with a simulated plastic deformation of the leading edge. The modules of elasticity have been reduced to 5 000 kp/mm<sup>2</sup> and 10 000 kp/mm<sup>2</sup> for the elements close to the leading edge. In this way only a smaller part of the loads is transformed into membrane stresses. Now the maximum blade stresses appear at the 20% chord also on the parent propeller. The difference between the propeller in [17] and the parent propeller is mainly the blade shape and the camber. These parameters can obviously be important for the distribution of stresses in the propeller blade.

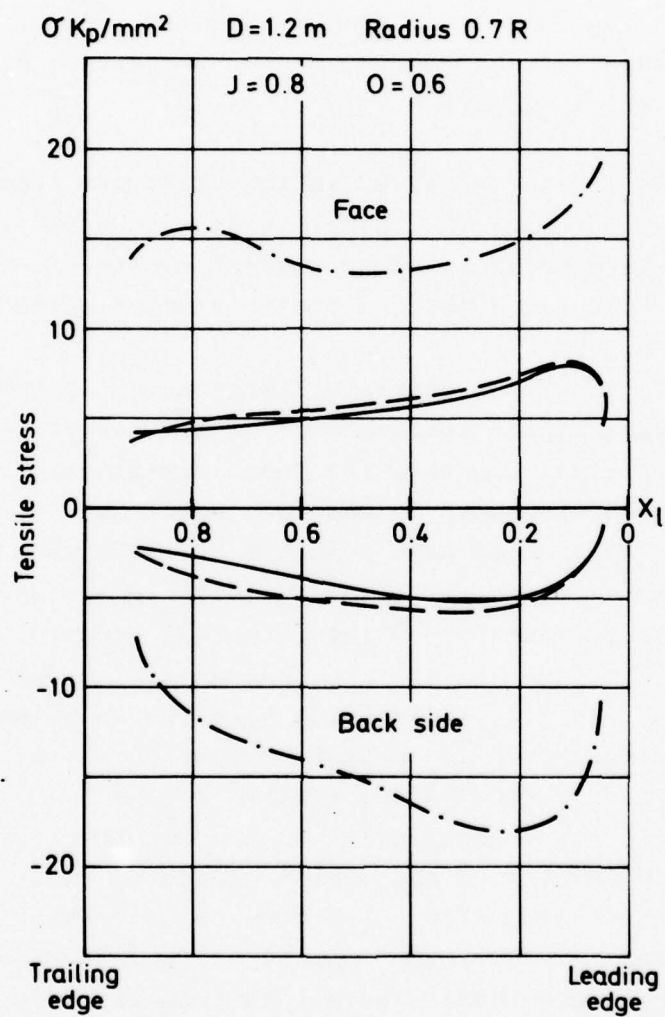
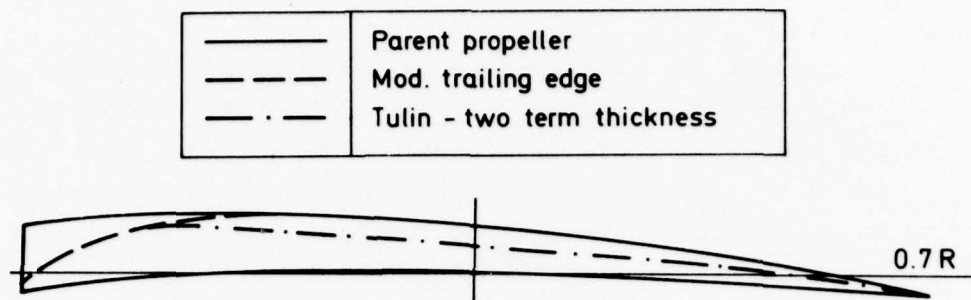


Fig 13. Effect of profile modification on maximum principal stresses



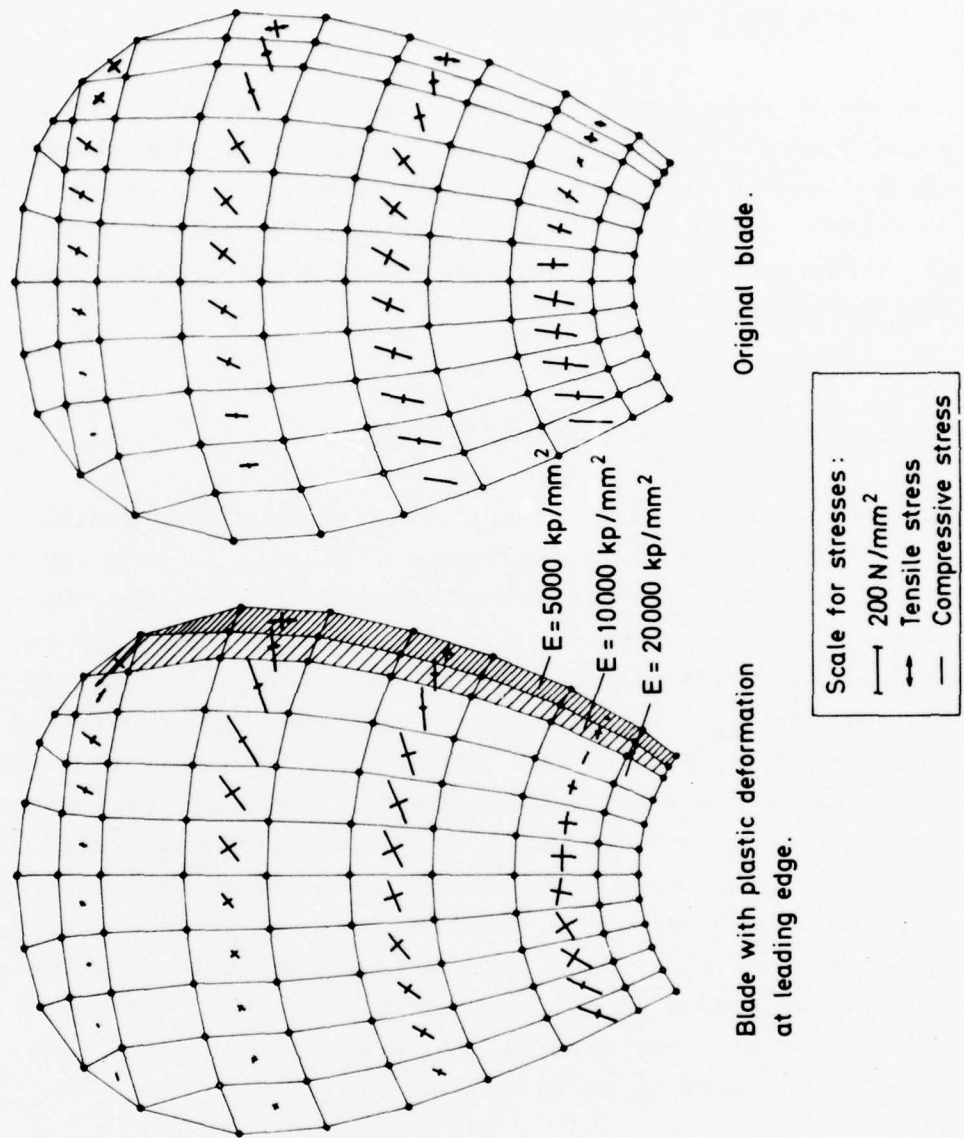


Fig 14. Stresses on suction side of parent propeller blade. Influence of plastic deformation of the leading edge

## 12. INFLUENCE OF SHAFT INCLINATION AND CLEARANCE TO BOTTOM AND RUDDER

Systematic propeller data from tests in homogeneous flow are often used for design of propellers for small high-speed craft. The agreement with full scale results is however sometimes rather poor [13]. The reason for this is often the influence of shaft inclination and small clearance to boat bottom and rudder.

### 12.1 INFLUENCE OF SHAFT INCLINATION

All propellers in the systematic series have been tested also at 8 degrees shaft inclination. In Fig 15 some typical trends for the parent series are shown. Results for two advance ratios are shown.  $J_F$  is the advance ratio for incipient face cavitation at  $\sigma = 0.6$  in homogeneous flow. In the same way  $J_{sc}$  is the advance ratio when the propeller is supercavitating at  $\sigma = 0.6$ . Results for non-cavitating condition and  $\sigma = 1.0$  and  $0.5$  are shown. For small cavitation numbers the typical influence is a few per cent increase in thrust and efficiency. The torque is however not influenced very much. The effect is stronger for high advance ratios ( $J_F$ ) than for lower ( $J_{sc}$ ). Tests with conventional propellers in cavitation tunnel have shown results of the same magnitude [12]. The results are, however, not quite consistent with results shown in [1].

### 12.2 INFLUENCE OF VERTICAL CLEARANCE

For a heavily cavitating propeller the vicinity to a solid boundary like the boat bottom can influence the propeller characteristics. Results of tests with a supercavitating propeller with different vertical clearances to a plane above the propeller are shown in Fig 16.

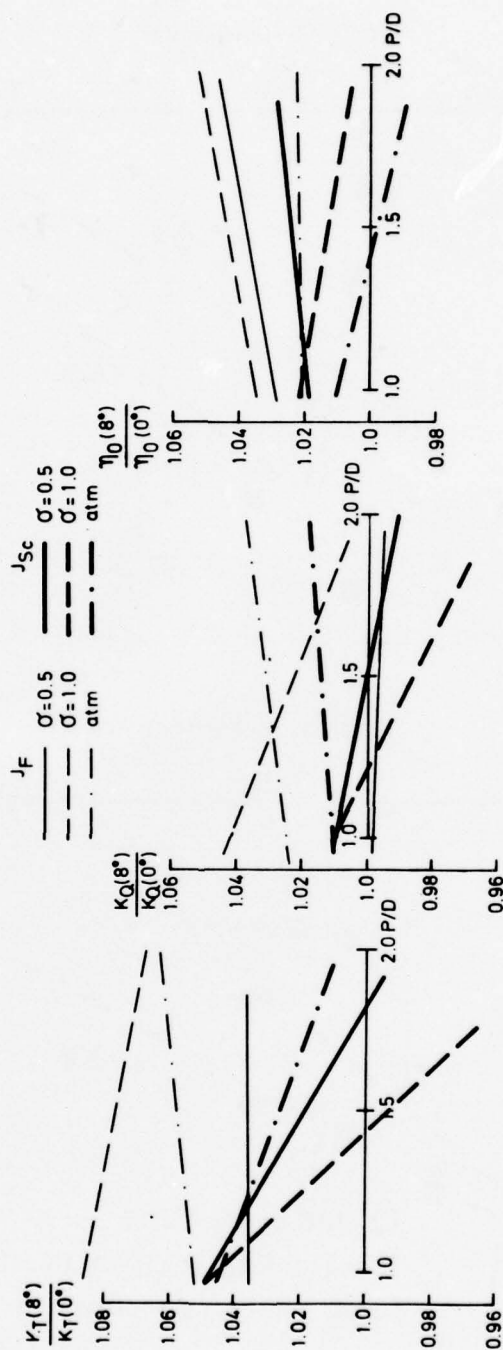


Fig 15. Influence of shaft inclination

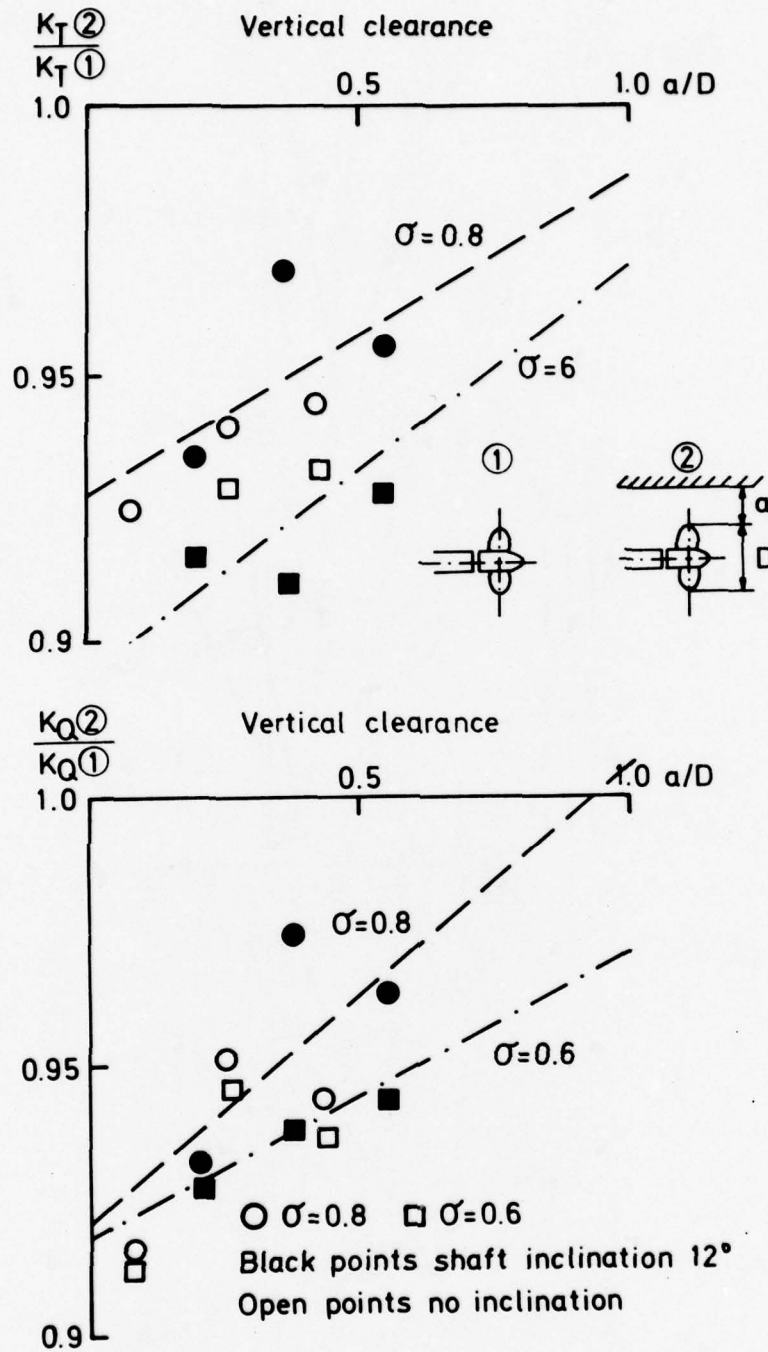


Fig 16. Influence of clearance to bottom.  
 $J = 0.95$   $P/D = 1.4$



Tests were carried out in homogeneous flow and with 12 degrees shaft inclination. As shown in Fig 16, the results showed a considerable scatter. The trend is, however, quite clear. Thrust and torque are reduced when the clearance is reduced. Shaft inclination does not seem to modify this effect. Accordingly, for each cavitation number, a common mean line has been drawn for all the points using the method of least squares. A vertical clearance of about one propeller diameter seems to be necessary in order to avoid this reduction of thrust and torque.

### 12.3 INFLUENCE OF RUDDER ARRANGEMENT

With a rudder located in the propeller slipstream the propeller influence on the rudder characteristics is large. If, however, the rudder is mounted close to the propeller, also the rudder influence on the propeller characteristics is considerable. In Fig 17 some results from the cavitation tunnel are shown. The height of the rudder was about one propeller diameter and the mean chord was  $1.7 \cdot D$ . The thickness/chord ratio for the tested rudder was about 10 per cent. As shown in Fig 17, the rudder has caused an increase of both thrust and torque. The effect is more pronounced when the rudder is close to the propeller and for the cavitating propeller. All tests showed a small increase in efficiency, probably due to a reduction of the rotational losses in the slipstream. In [14] a very small rudder (height less than half the propeller diameter) was tested close to the propeller and here almost no effect was registered. In [15] results of the same magnitude as in Fig 17 were shown.

Tests with two rudders located behind the propellers but placed beside the slipstream showed quite different results. Under these conditions thrust, torque and efficiency for the propeller were reduced by a few per cent instead.

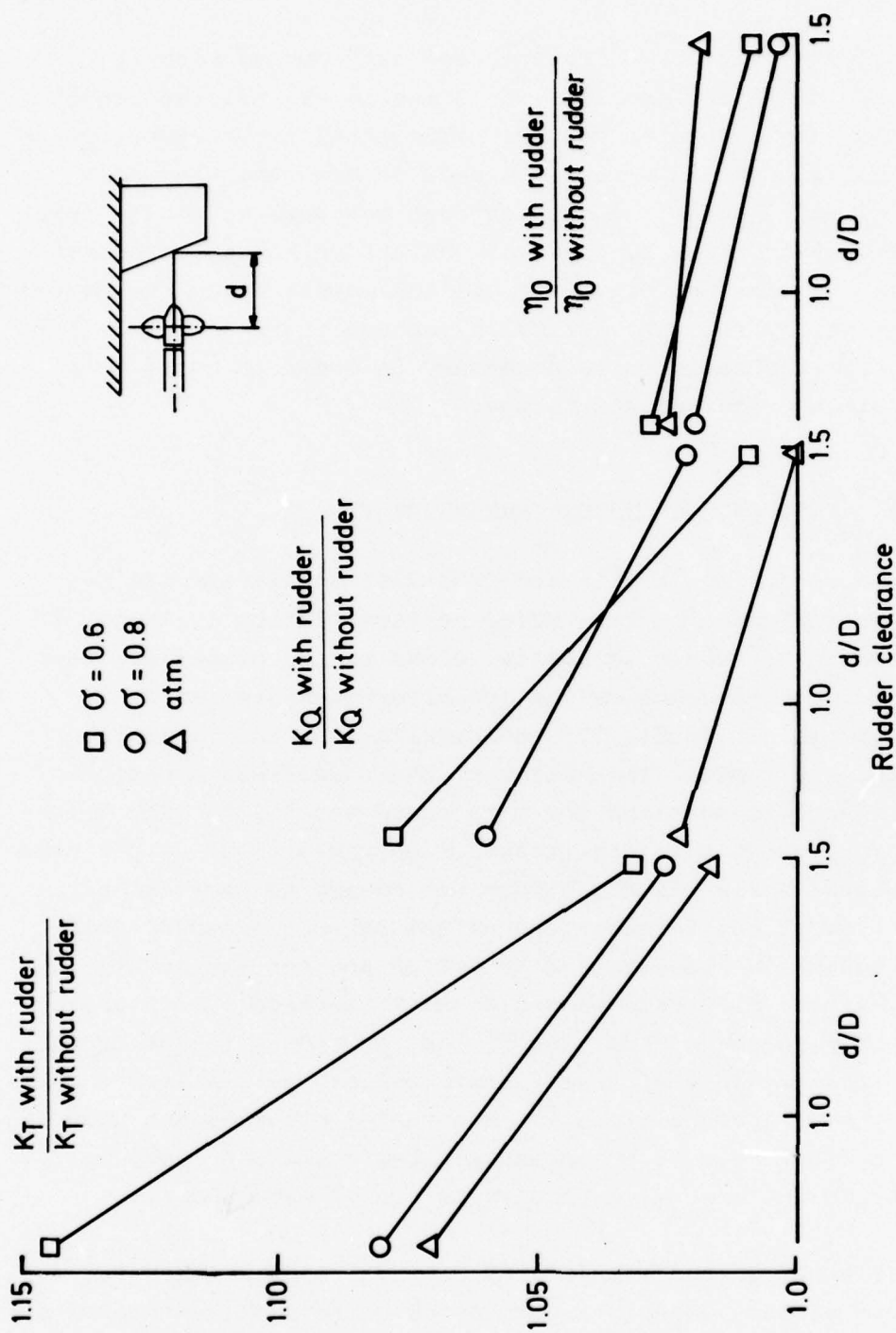


Fig 17. Influence of clearance to rudder.  
 $J = 0.95$   $P/D = 1.4$

# INFLUENCE OF ARRANGEMENT ON CENTER PROPELLER THRUST


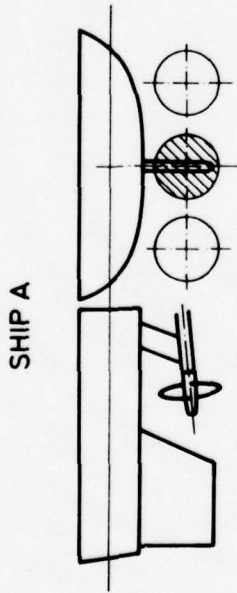
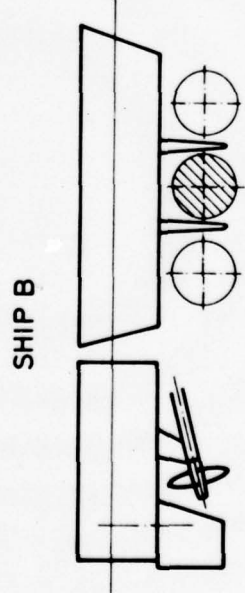
	SHAFT INCL.	HULL	RUDDERS	TOTAL
	100 %	100 %	100 %	100 %
	98 %	92 %	109 %	98 %
	94 %	91 %	94 %	80 %

Fig 18. Influence of different arrangements on propeller thrust

## 12.4 INTEGRATED EFFECT

When making propeller designs for high speed ships with heavily or supercavitating propellers it is very important to test the propeller with the complete arrangement. This is verified by examples where almost the same propeller was tested in full scale with quite different results. An examination of the propeller arrangements, which were entirely different for the two propellers, gave the results according to Fig 18 at model tests.

The results of Fig 18 agree very nicely with the results of the measured mile tests in full scale which gave 1.0 for ship A and 0.82 for ship B, compared with tests in homogeneous flow.

## 13. COMPARISON WITH FULL SCALE OBSERVATIONS

Full scale tests with observations of cavitation are important for the development of model testing technique. On the Spica class torpedo boats very thorough full scale tests have been carried out. The tests included cavitation observations, thrust and torque measurements and measurements of pressure fluctuations and vibrations.

In Fig 19 comparisons of the cavitation patterns in full scale and at model tests are shown. At model tests it was observed that for partially cavitating propellers a small roughening of the surface, created by painting the propeller with a thin spray paint, can change the cavitation pattern considerably. The cavitation of the painted propeller is shown to consist of smaller bubbles than that of the polished propeller. When the propeller sections are working near shock-free entrance the cavitation extension is larger for the painted propeller than for the unpainted one. When the propellers are near or at supercavitation the differences are small (compare  $J = 1.1$  and  $J = 1.0$  in Fig 19). The cavitation pattern in full scale is shown to consist of



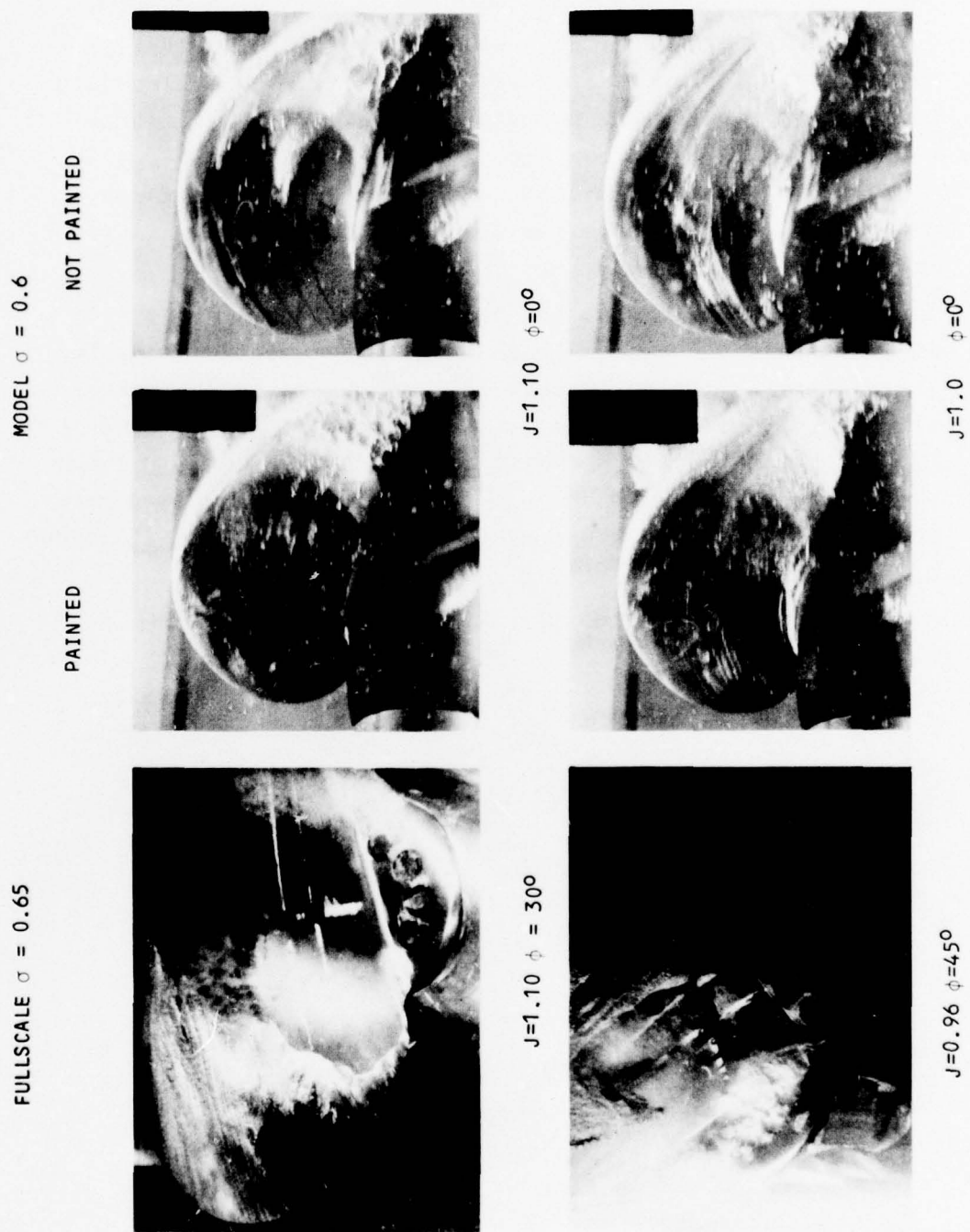


Fig 19. Comparison of cavitation photographs.  
Full scale - model tests in homogeneous flow.

small bubbles in a similar way as the cavitation on the painted propeller.

The model tests were run at Reynolds numbers at 0.7 radius of about  $3.5 \cdot 10^6$  and the full scale tests at about  $2 \cdot 10^7$ . The reasons for differences in cavitation pattern is believed to be due to the different boundary layers. With a slightly roughened surface the boundary layer at the model tests creates more full scale-like cavitation at large advance ratios. Similar scale effects for the Newton Rader series are indicated in [16].

Cavitation extensions at the full scale tests are compared with extensions at model tests with corresponding propeller arrangement as the full scale ship (same shaft inclination, same relative clearance to bottom and rudder). Unfortunately the photographs from the model tests were not very good and the extensions are better compared from the sketches according to Fig 20. The agreement between the extensions is shown to be rather good.

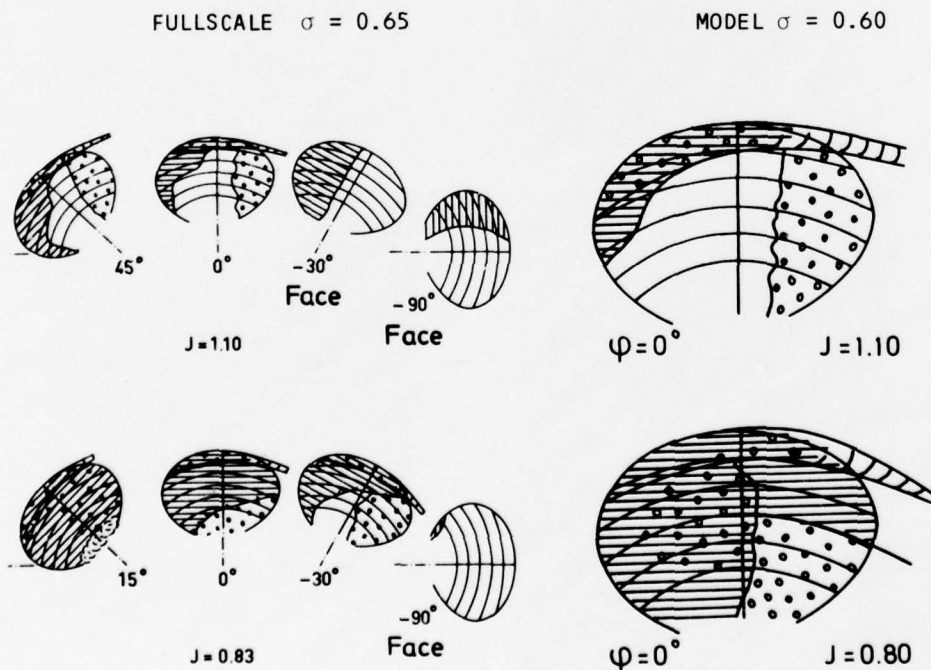


Fig 20. Comparison of cavitation extensions. Full scale - model tests with complete arrangement

Measurements of thrust and torque from these tests are compared in Fig 21. In full scale the variation in propeller loading at constant speed was achieved by varying the thrust between the center- and the wing -propellers. (The ship has three propellers). The agreement between full scale and model tests is shown to be rather good for the center propeller at medium loadings. This was also the propeller simulated at the model tests. The full scale tests with lightly loaded center propeller gave obviously misleading results, probably due to negative wake fraction caused by the race of the highly loaded wing propellers.

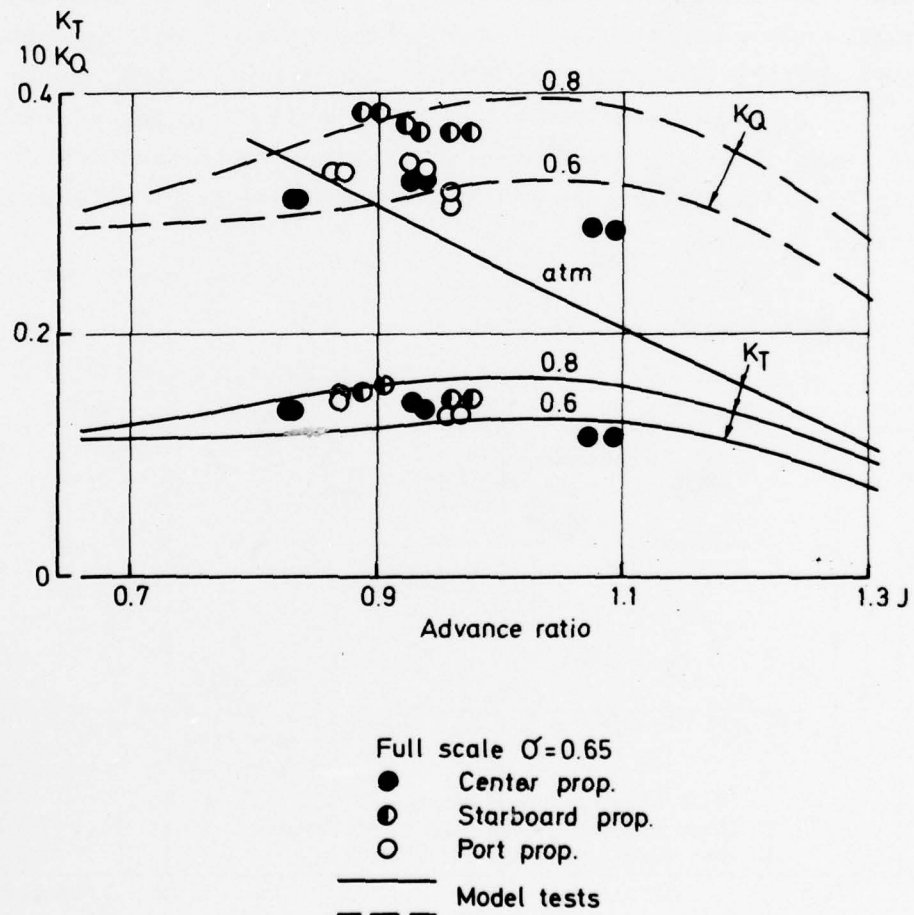


Fig 21. Comparison of propeller characteristics.  
Full scale - model tests with complete arrangement

## 14. MEASUREMENTS OF PRESSURE FLUCTUATIONS

Also the pressure fluctuations in the plate above the propeller were measured at the model tests. Comparison of these results with full scale results are shown in Fig 22.

The non-dimensional amplitudes at the model tests are shown to be somewhat smaller in the high speed range than those of the full scale tests. The reason for this could be that only the center propeller was present at the model tests.

At the model tests also an equivalent propeller of conventional design was tested. In the high speed range this propeller excites only about half the amplitudes of the supercavitating propeller. Thus the supercavitating propeller is favourable from erosion point of view but the vibration excitation forces are considerably higher than for a conventional propeller.

$$K_p = \frac{2p}{\rho n^2 D^2} \quad \text{Dimensionless pressure amplitude}$$

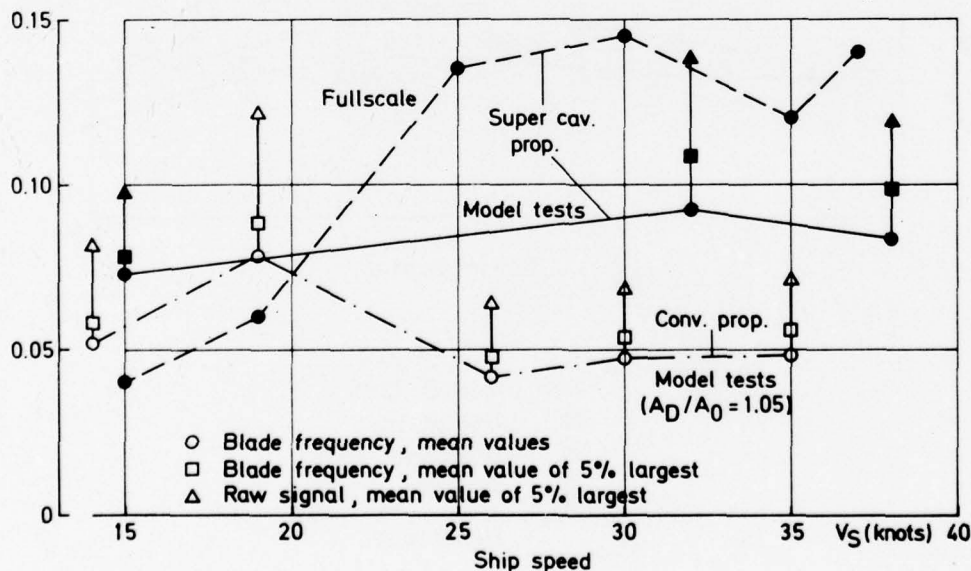


Fig 22. Comparison of pressure fluctuations in boat bottom. Full scale - model tests with complete arrangement



## 15. CONCLUSIONS

The purpose of the systematic series was:

1. to form the basis for a good prediction of propeller performance
2. to show the influence of different design parameters on the performance
3. to show the interaction between propeller, rudder and hull

As shown above, these goals have been reached in the following way:

1. Design of a propeller with the geometry of the parent series can be made according to Figs 2-4 and the Appendix of this paper
2. The cavitation performance can be predicted by the use of Figs 5, 6
3. Design of a propeller with another geometry can be made according to [2], corrected for cavity-blade interference effect of Fig 7
4. Influence of design parameters as hub diameter, design thrust and blade area ratio are shown in Figs 8, 9
5. The requirement for an efficient erosion free propeller at low speeds  $\sigma \leq 0.8$  is well fulfilled by a propeller from the parent series
6. The performance of a heavily cavitating propeller is influenced by interaction with rudder and hull and also by shaft inclination. To get a reliable prediction of the performance it is necessary to test the complete propeller arrangement
7. At partially cavitating conditions the cavitation patterns and thrust and torque are influenced by the boundary layer on the blades. Full scale-like cavitation patterns at model tests are obtained with propellers with a slightly roughened surface
8. Pressure fluctuations induced by a supercavitating propeller are considerably higher than those induced by a propeller of conventional type.

## 16. ACKNOWLEDGEMENTS

The author wishes to express his gratitude to the Naval Material Department of the Defence Material Administration of Sweden for sponsoring the present investigation and to Dr Hans Edstrand, Director General of SSPA for the opportunity to carry out the study. The author also wishes to thank Mr Carl-Anders Johnsson for initiating the systematic series and for all encouraging discussions during the investigation. Thanks are also due to those members of the staff at SSPA who took part in the work.

## 17. REFERENCES

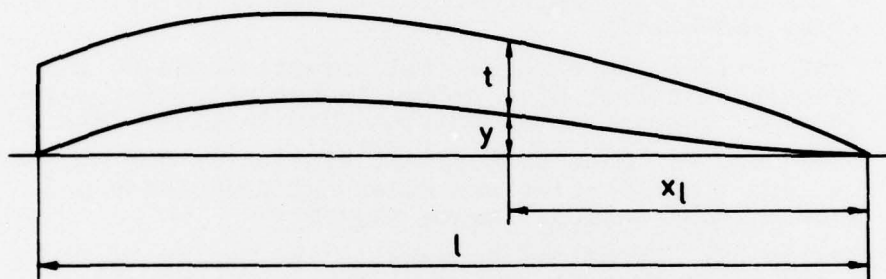
- [1] Newton, R and Rader, H: Performance Data for High-Speed Craft. Trans The Royal Institution of Naval Architects, 1961
- [2] Venning, E and Habermann, W: Supercavitating Propeller Performance. Trans SNAME 1962
- [3] Kramer, K: Induzierte Wirkungsgrade von Best-Luftschrauben endlicher Blattzahl. Luftfahrtforschung B 115 1938
- [4] Tachmindji, A, Morgan, W: The Design and Estimated Performance of a Series of Supercavitating Propellers. Proceedings of the Second Symposium on Naval Hydrodynamics, 1958
- [5] Lindgren, H and Johnsson, C-A: Propeller Calculations using Vortex Theory, Diagrams and Example of Calculation. SSPA Allmän Rapport Nr 2 1956
- [6] Edstrand, H: The Cavitation Laboratory of the Swedish State Shipbuilding Experimental Tank. SSPA circular No 32 1974
- [7] Cox, G: State-of-the Art for Supercavitating Propeller Design Methods. Appendix IV of the 12th ITTC Propeller Committee. Report 1968
- [8] Tulin, N: Supercavitating Propellers - History, Operating Characteristics and Mechanics of Operation. Proceedings of the fourth Symposium on Naval Hydrodynamics, 1962

- [9] Rutgersson, O: Propellers SSPA-FMV series K131. Summary of cavitation properties for propellers 3.105, 3.075 and 3.050. SSPA Report K131-24, 1974 (in Swedish)
- [10] Johnsson, C-A: Propeller design aspects of large high powered ships. Symposium on High powered propulsion of large ships. Wageningen 1974
- [11] Mechanics Research, Inc Stardyne, Control Data Corp. Users Manual Sept 1972
- [12] Peck, J and Moore, D: Inclined-shaft propeller performance characteristics. NSRDC Report 4127, 1974
- [13] Blount, D and Hankley, D: Full Scale Trials and Analysis of High-Performance Planing Craft Data. Trans SNAME 1976
- [14] Suhrbier, K: An experimental investigation on the propulsive effect of a rudder in the propeller slipstream. International Shipbuilding Progress Febr 1974
- [15] Grollius, W: Untersuchung des Einflusses der Wechselwirkung von Propeller und Ruder auf Propulsion und Schwingungserregung. Hansa May 1974
- [16] Kruppa, C: Practical Aspects in the Design of High-Speed small Propellers. International Shipbuilding Progress 1976
- [17] Davis, B.V. and English, J.W: The Evolution of a Fully Cavitating Propeller for a High-Speed Hydrofoil Ship. Proceedings on the 7th ONR Symposium on Naval Hydrodynamics 1968

## APPENDIX

### GEOMETRY AND CHARACTERISTICS OF THE PARENT SERIES

The geometry of the parent propeller series SC 3.050 is briefly described in chapter 3. The more exact geometry and the propeller characteristics are, however, shown in this Appendix. The profile shape with the "three term" face and the "two term modified" thickness distribution is defined in Table 2, equation (1) and Figs 23 and 24.



Distance from leading edge $x_l$	Face Camber "3-term" $y/y_{\max}$	Profile thickness $t(x_l) = C_L l C(x_l) + \alpha l D(x_l)$ (1)	
		$C(x_l)$	$D(x_l)$
0	0	0	0
0.025	0.01547	-0.0075	0.0031
0.05	0.03324	-0.0168	0.0057
0.1	0.08825	-0.0395	0.0101
0.2	0.25903	-0.0789	0.0173
0.3	0.47851	-0.0975	0.0222
0.4	0.69628	-0.0929	0.0246
0.5	0.88252	-0.0718	0.0257
0.6	0.98453	-0.0378	0.0259
0.7	0.98567	0.0059	0.0256
0.8	0.83954	0.0569	0.0247
0.9	0.52034	0.1121	0.0230
0.95	0.28769	0.1396	0.0220
1.0	0	0.1670	0.0209

Table 2. Profile shape



Radius x	1.0	0.95	0.9	0.8	0.7
$\frac{1a}{D} = \frac{1f}{D}$	0	0.1291	0.1591	0.1825	0.1845

Radius x	0.6	0.5	0.4	0.3	0.25
$\frac{1a}{D} = \frac{1f}{D}$	0.1791	0.1700	0.1600	0.1491	0.1441

Table 3. Blade shape of the parent series  $x_h = 0.19$

The blade shape is tabulated in Table 3.

The interpolated propeller characteristics of the parent series at  $\sigma = 0.4, 0.6$  and  $0.8$  are shown in Figs 25-33.

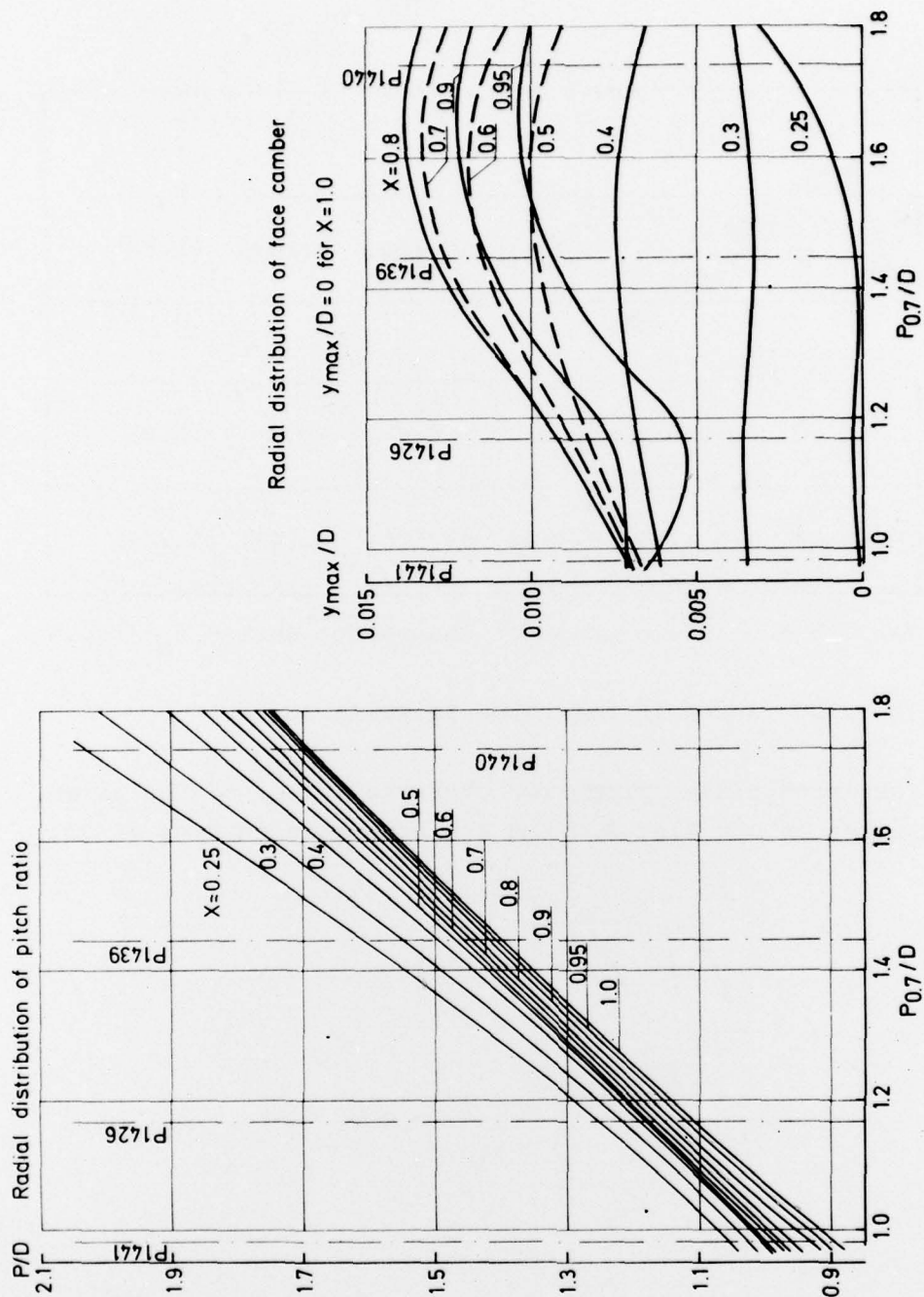


Fig 23. Parameters defining the profiles of the parent series. Pitch ratio and face camber

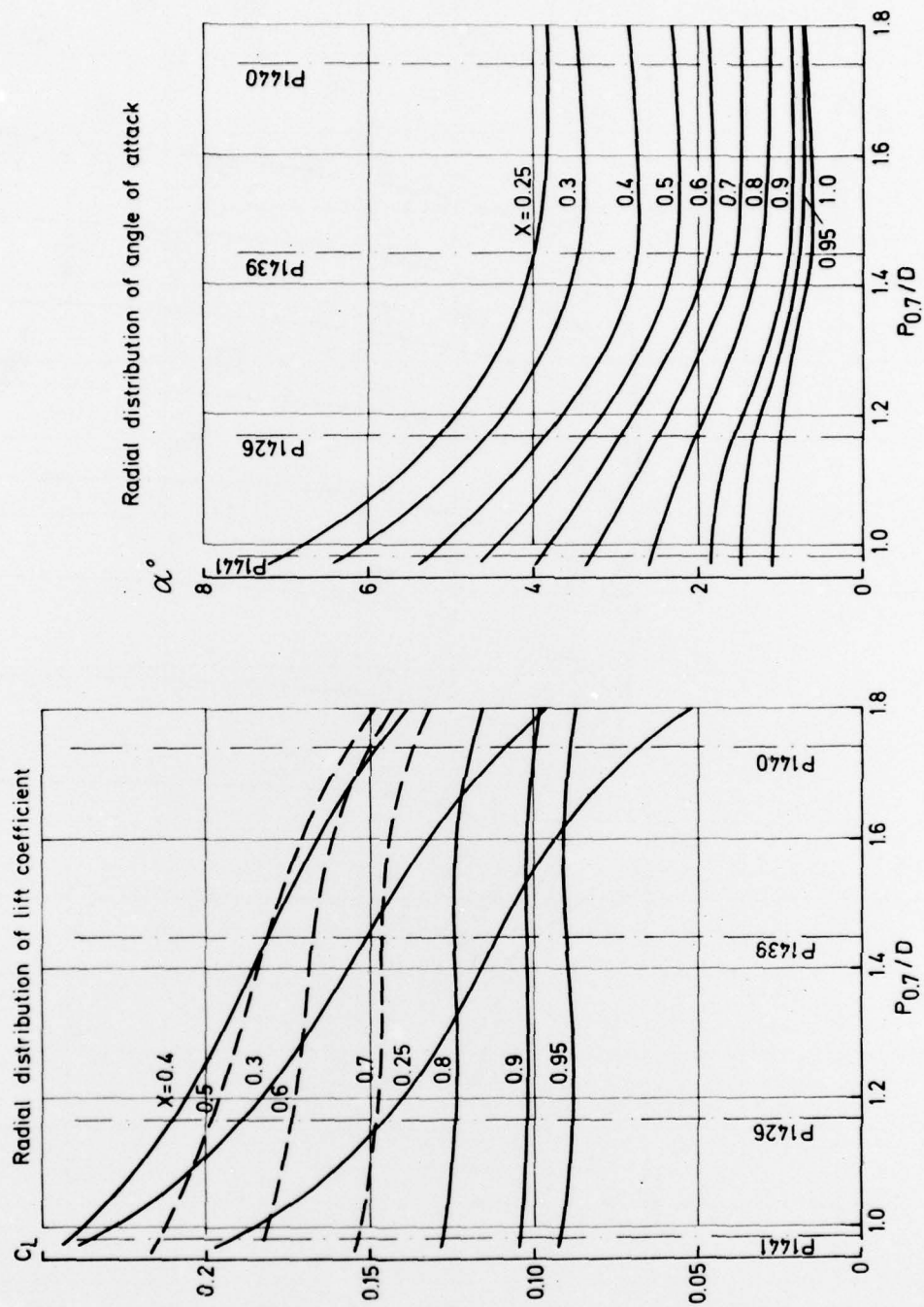


Fig 24. Parameters defining the profile thickness.  
Lift coefficient and profile angle of attack

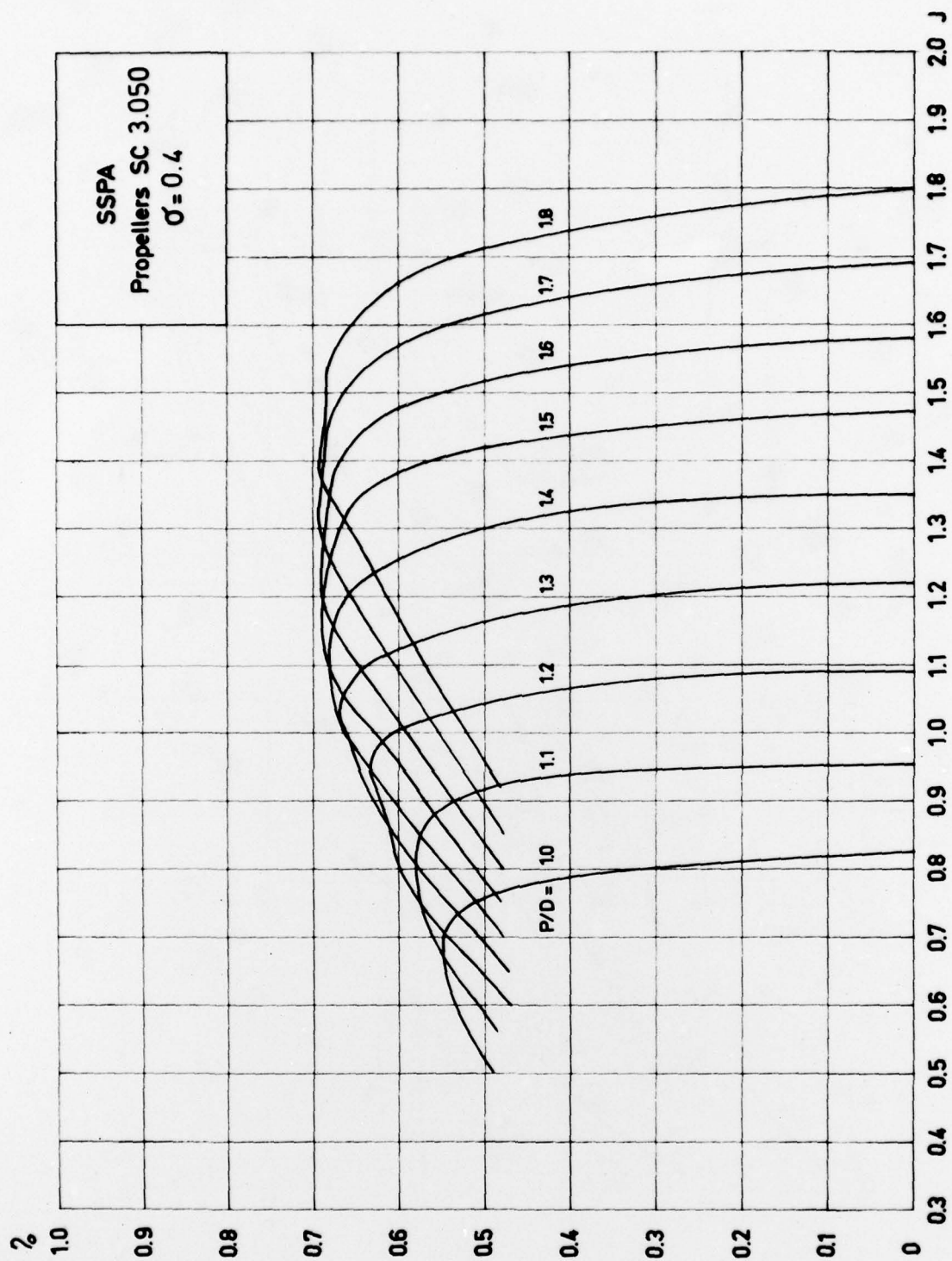


Fig 25. Propeller characteristics for parent series  
at  $\sigma = 0.4$ .



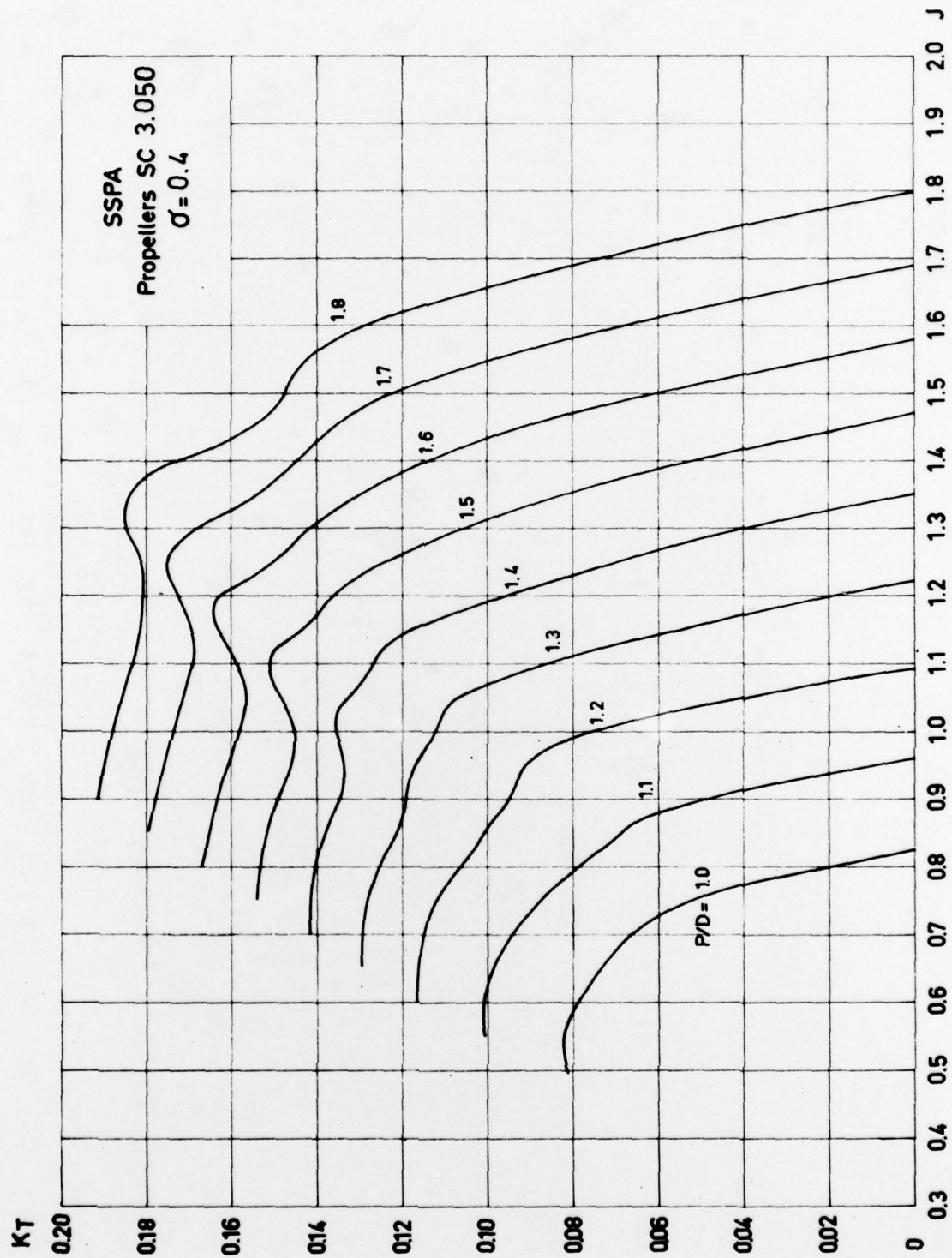


Fig 26. Propeller characteristics for parent series  
at  $\sigma = 0.4$  Thrust coefficient

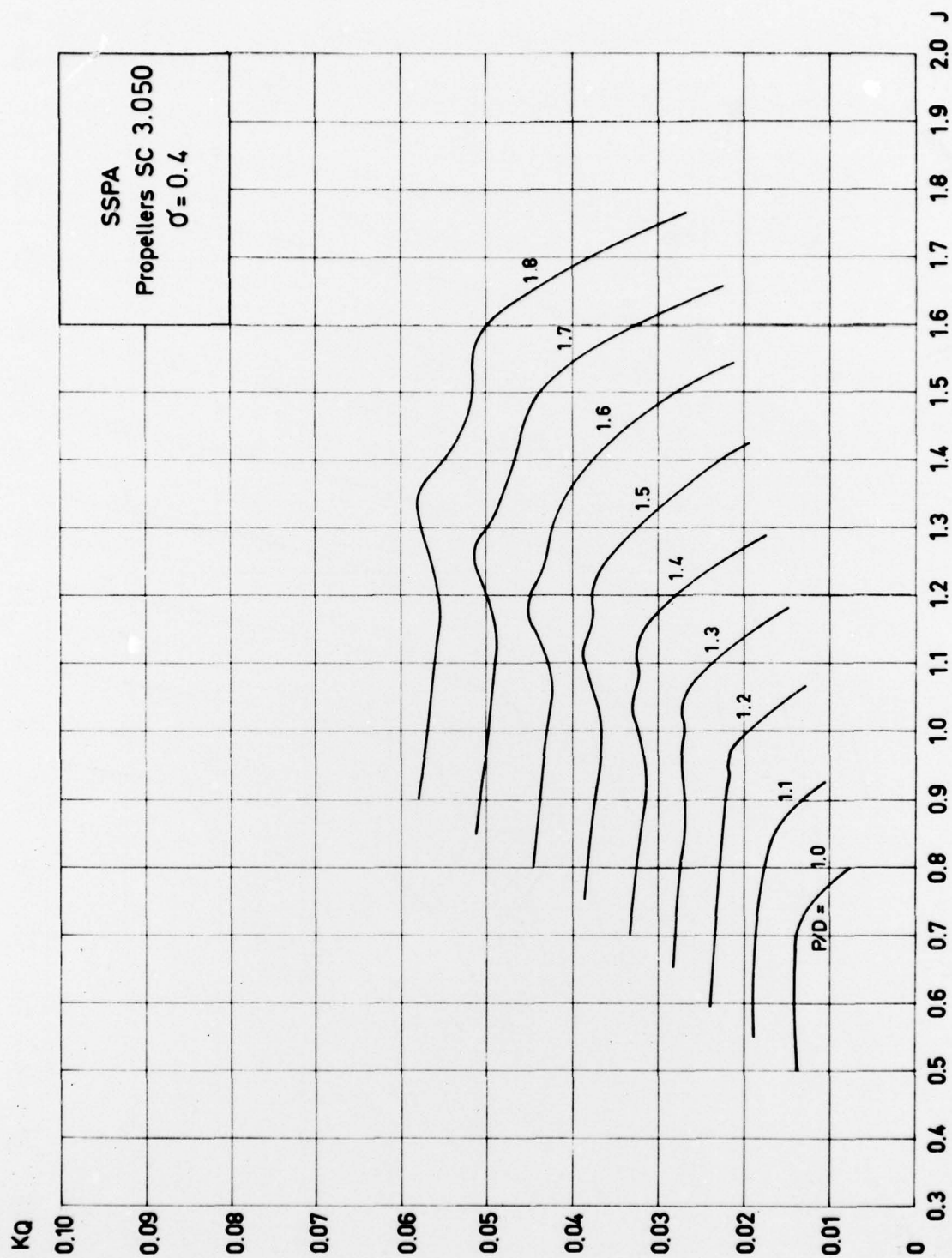


Fig 27. Propeller characteristics for parent series  
at  $\sigma = 0.4$  Torque coefficient

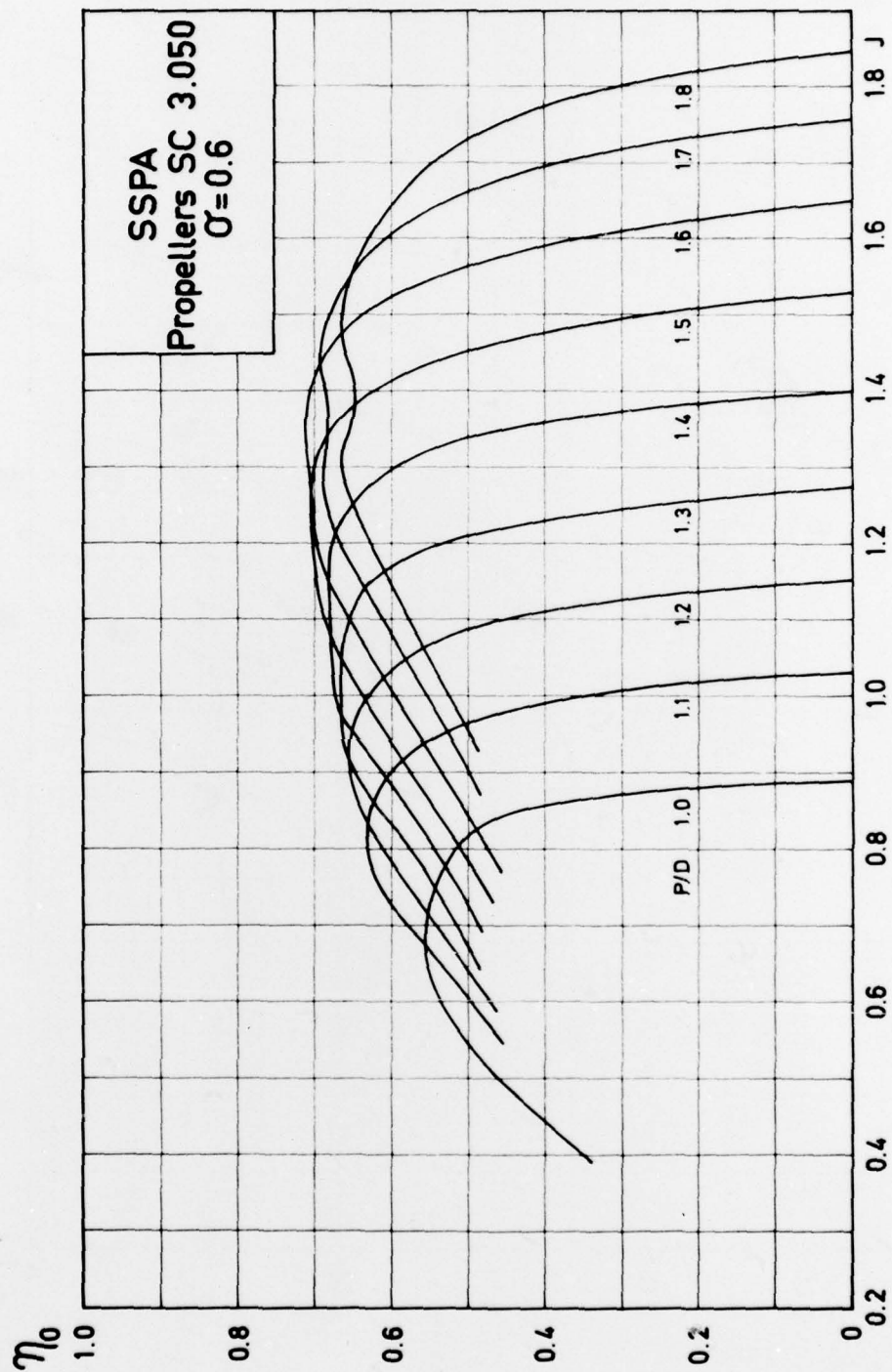


Fig 28. Propeller characteristics for parent series  
at  $\sigma = 0.6$ . Efficiency

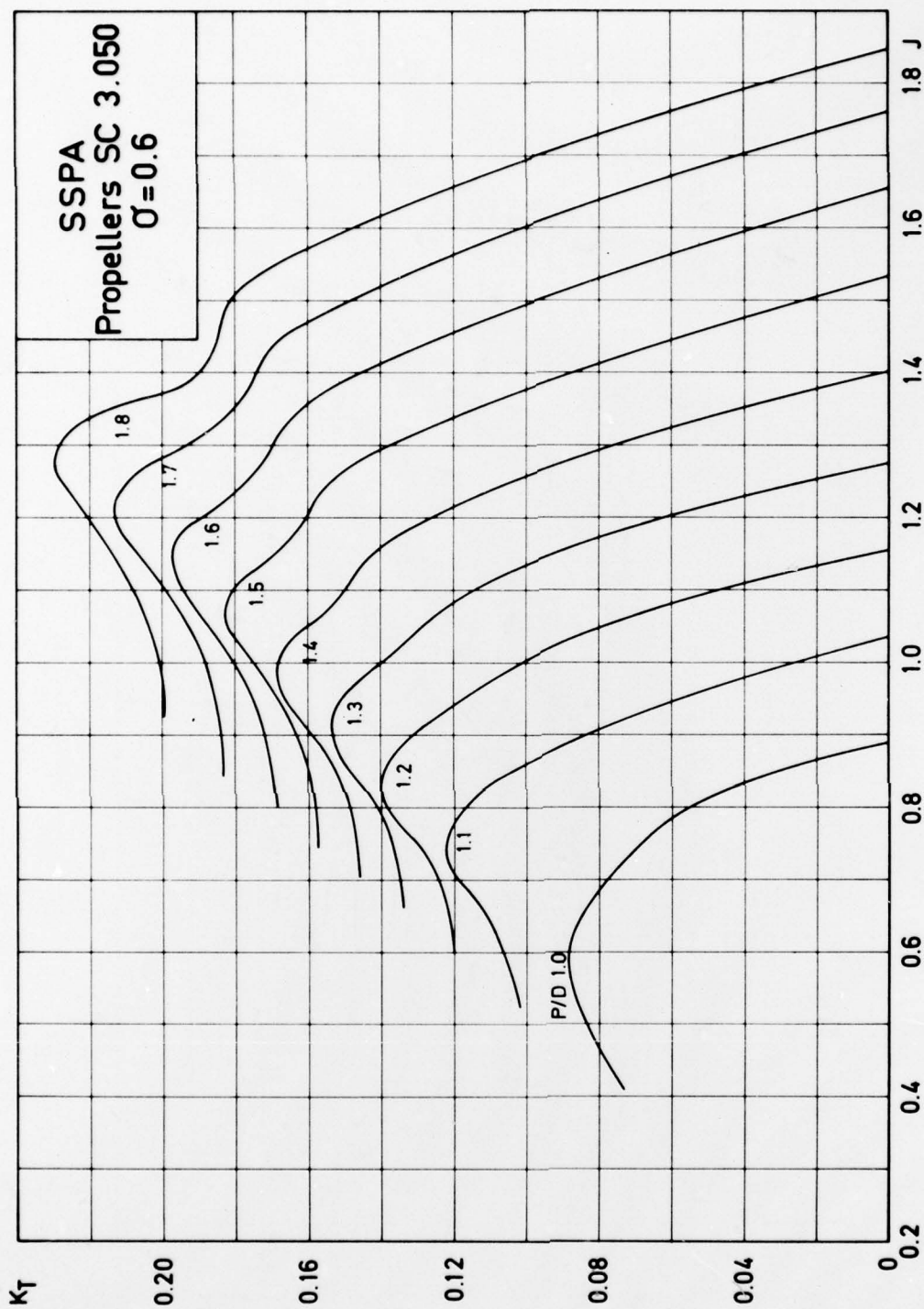


Fig 29. Propeller characteristics for parent series  
at  $\sigma = 0.6$ . Thrust coefficient



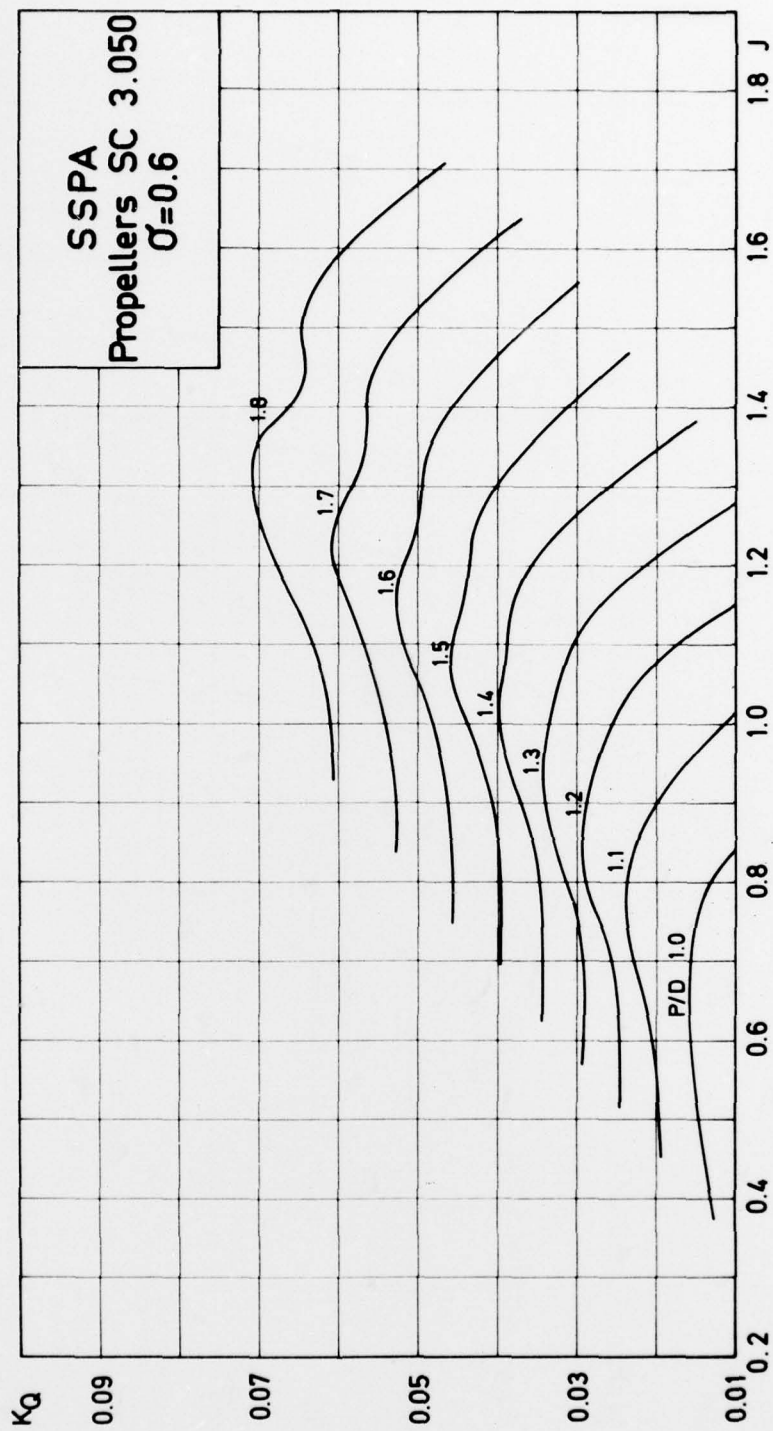


Fig 30. Propeller characteristics for parent series  
at  $\sigma = 0.6$  Torque coefficient

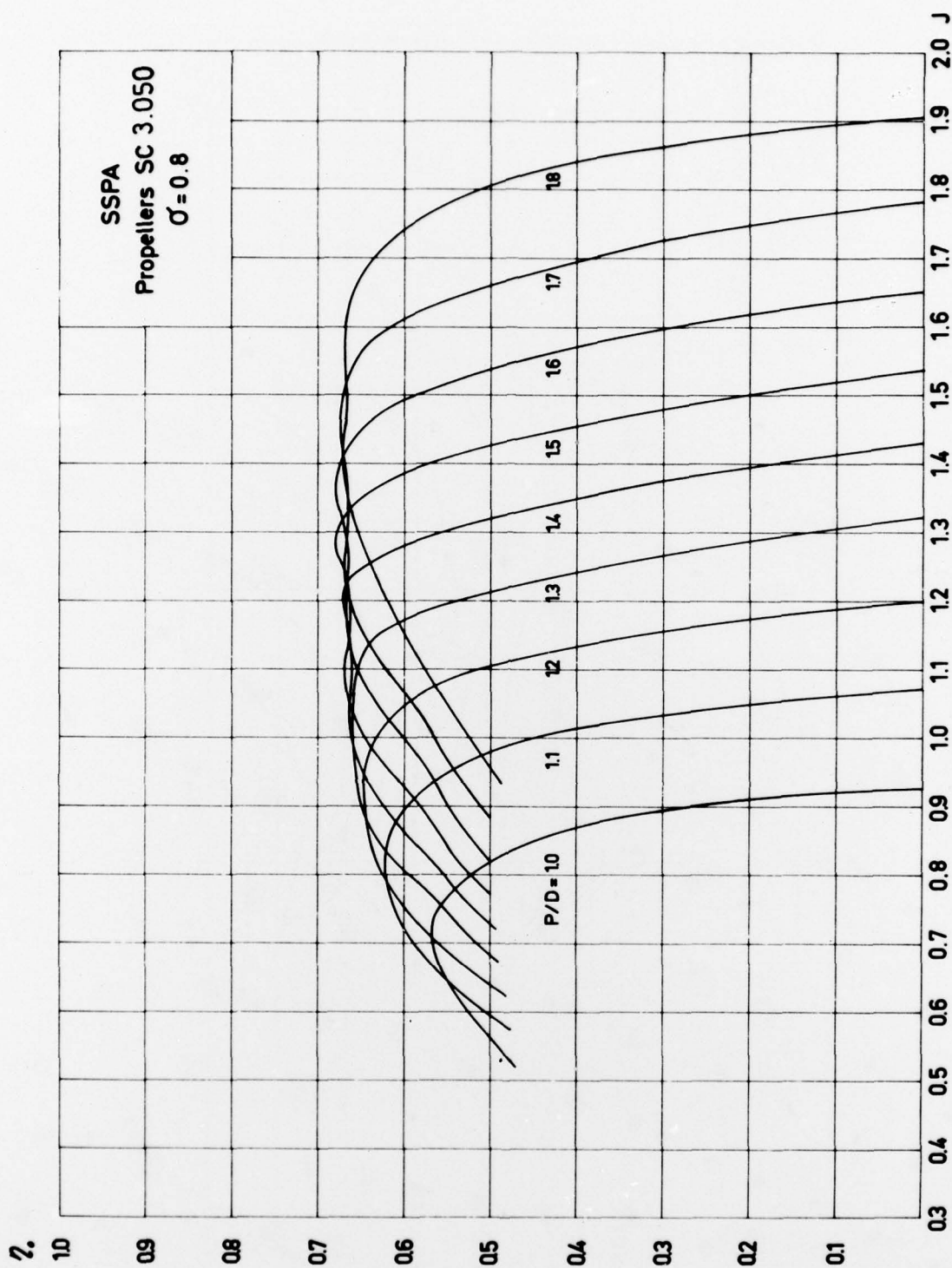


Fig 31. Propeller characteristics for parent series  
at  $\sigma = 0.8$ . Efficiency

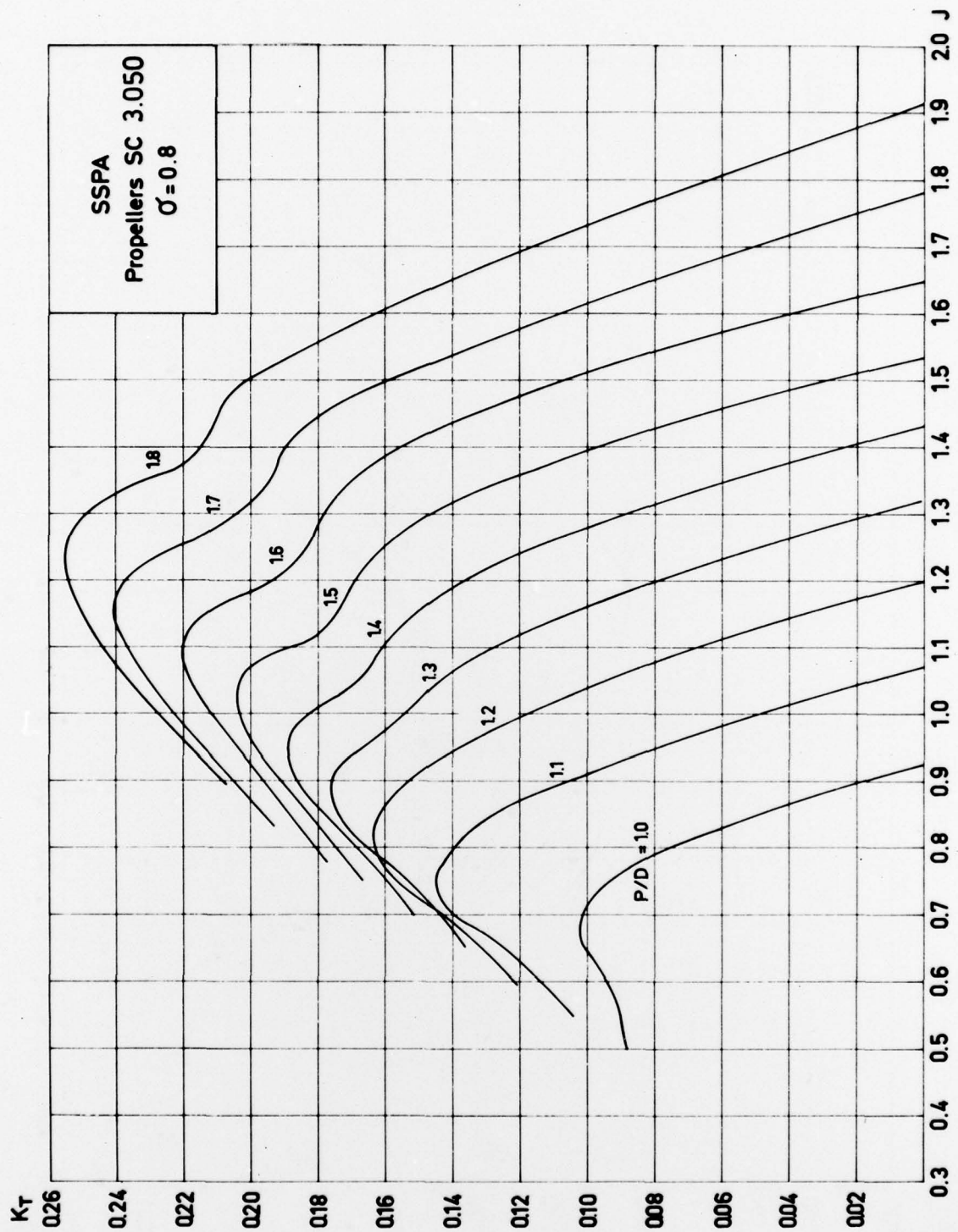


Fig 32. Propeller characteristics for parent series  
at  $\sigma = 0.8$  Thrust coefficient

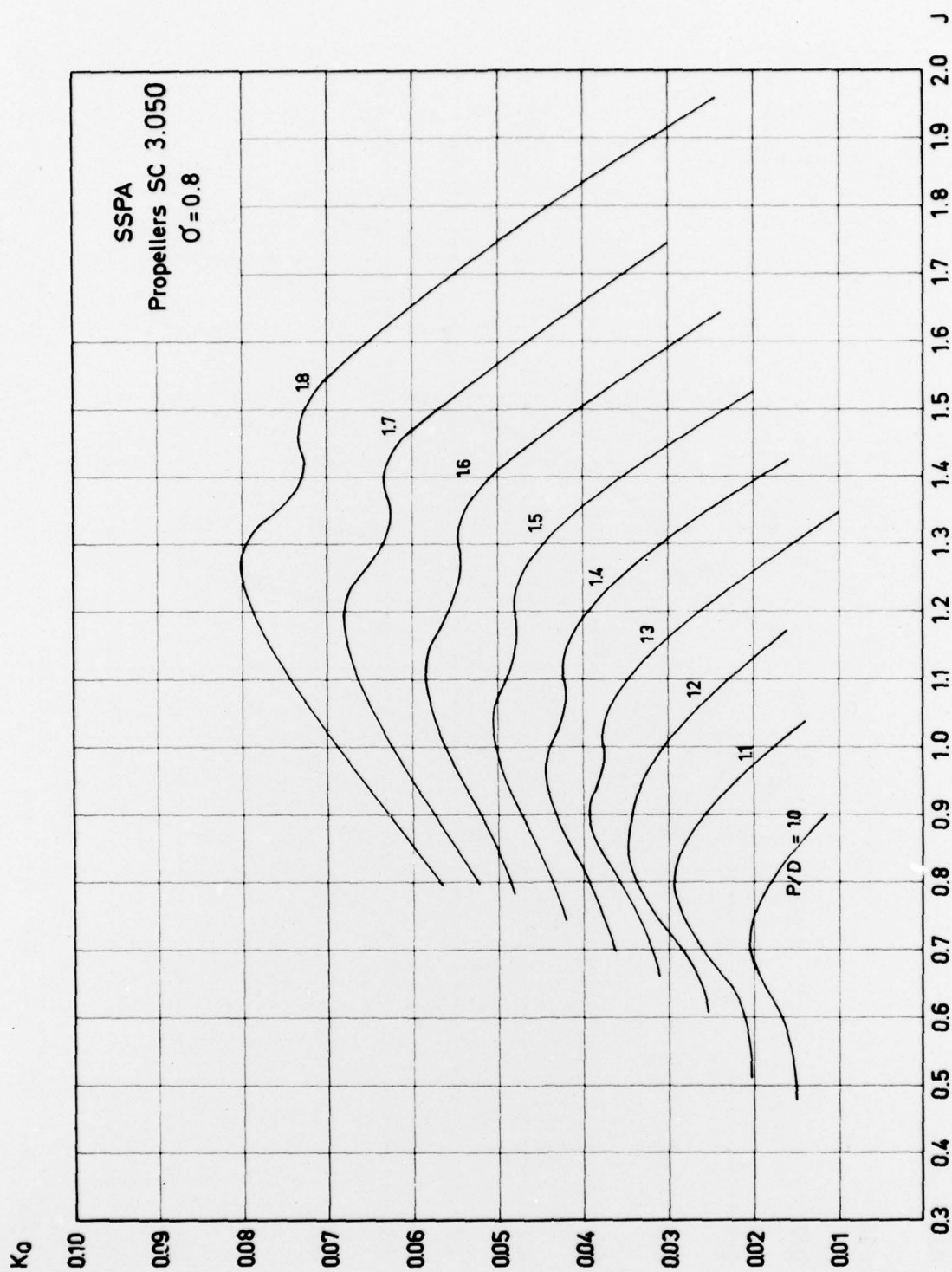


Fig 33. Propeller characteristics for parent series  
at  $\sigma 0.8$  Torque coefficient



Forts. från omslagets 2:a sida [Continued from inside front cover].

47. Model Tests with a Family of Three and Five Bladed Propellers, av HANS LINDGREN, 1961.
48. Cavitation Tunnel Tests with Merchant Ship Propellers, av HANS LINDGREN, 1961.
49. Influence of V and U Shaped Fore Body Sections on Motions and Propulsion of Ships in Waves, av BENGT BENGTTSSON, 1962.
50. An Examination of Some Theoretical Propeller Design Methods, av C.-A. JOHNSON, 1962.
51. Mathematical Representation of Bodies of Revolution by Use of a Digital Computer, av ÅKE WILLIAMS, 1962.
52. Comparison of Propeller Design Techniques, av C.-A. JOHNSON, 1963.
53. Circle Tests with a Radio-Controlled Model of a Cargo Liner, av NILS H. NORRBIN, 1963.
54. Ship Trial Analysis and Model Correlation Factors av HANS LINDGREN, 1963.
55. Mathematical Representation of Ordinary Ship Forms, av ÅKE WILLIAMS, 1964.
56. Influence of V and U Shaped Fore Body Sections on Motions and Propulsion of Ships in Waves at Ballast Draught, av BENGT G. BENGTTSSON, 1965.
57. Forces in Oblique Towing of a Model of a Cargo Liner and a Divided Double-Body Geosim, av NILS H. NORRBIN, 1965.
58. Cavitation Inception on Head Forms. ITTC Comparative Experiments, av HANS LINDGREN och C.-A. JOHNSON, 1966.
59. Future Design of Ship Lines by Use of Analogue and Digital Computers, av ÅKE WILLIAMS, 1966.
60. The SSPA Standard Propeller Family. Open Water Characteristics, av HANS LINDGREN och E. BJÄRNE, 1967.
61. Wake and Thrust Deduction at Extreme Propeller Loadings, av SV. AA. HARVALD, 1967.
62. A Method for the Design of Ducted Propellers in a Uniform Flow, av GILBERT DYNE, 1967.
63. An Experimental Verification of a Design Method for Ducted Propellers, av GILBERT DYNE, 1968.
64. On Theoretical Predictions of Characteristics and Cavitation Properties of Propellers, av C.-A. JOHNSON, 1968.
65. Systematic Tests with Small, Fast Displacement Vessels, Including a Study of the Influence of Spray Strips, av HANS LINDGREN och ÅKE WILLIAMS, 1969.
66. The SSPA Cargo Liner Series, Resistance, av ÅKE WILLIAMS, 1969.
67. The SSPA Cargo Liner Series, Propulsion, av ÅKE WILLIAMS, 1970.
68. Theory and Observations on the Use of a Mathematical Model for Ship Manoeuvring in Deep and Confined Waters, av NILS H. NORRBIN, 1971.
69. Pressure Fluctuations Around a Marine Propeller. Results of Calculations and Comparison with Experiment, av C.-A. JOHNSON, 1971.
70. Propeller Excitation and Response of 230 000 TDW Tankers, av C.-A. JOHNSON och T. SØNTVEDT, 1972.
71. On Threshold Pressures for the Onset of Bubble Growth, av BROR PERSSON, 1974.
72. Theoretical Investigation on the Dynamics of Cavitation Bubble Growth, av BROR PERSSON, 1974.
73. Analysis and Storing of Ship Propulsion Data, av ÅKE WILLIAMS, 1974.
74. Single- and Twin-Screw Propulsion of Tankers and Bulk Carriers, av ÅKE WILLIAMS, 1975.
75. The Identification of Linear Ship Steering Dynamics Using Maximum Likelihood Parameter Estimation, av KARLJOHAN ÅSTRÖM, NILS H. NORRBIN, CLAES G. KÄLLSTRÖM och LENNART BYSTRÖM, 1975.
76. An Experimental Investigation of the Three-Dimensional Turbulent Boundary Layer on a Ship Model, av LARS LARSSON, 1976.
77. A Calculation Method for Three-Dimensional Turbulent Boundary Layers on Ship-Like Bodies, av LARS LARSSON, 1976.
78. Vibration Excitation Forces From a Cavitating Propeller. Model and Full Scale Tests on a High Speed Container Ship, av C.-A. JOHNSON, O. RUTGERSSON, S. OLSSON och O. BJÖRHEDEN, 1976.
79. Influence of Ship Size, Afterbody Shape and Propeller Speed of Rotation on Propeller Performance, av GILBERT DYNE, 1977.
80. Some Recent Trends in Hull Forms for Merchant Ships, av ÅKE WILLIAMS, 1978.
81. Shallow Water Phenomena and Scale Model Research - Some First Experience from the SSPA Maritime Dynamics Laboratory, av HANS EDSTRAND och NILS H. NORRBIN, 1978.
82. Supercavitating Propeller Performance. Influence of Propeller Geometry and Interaction between Propeller, Rudder and Hull, av OLLE RUTGERSSON, 1979.